

A Liquid Xenon Time Projection Chamber for Astrophysics and Prospects for a Sensitive Dark Matter Experiment

Elena Aprile

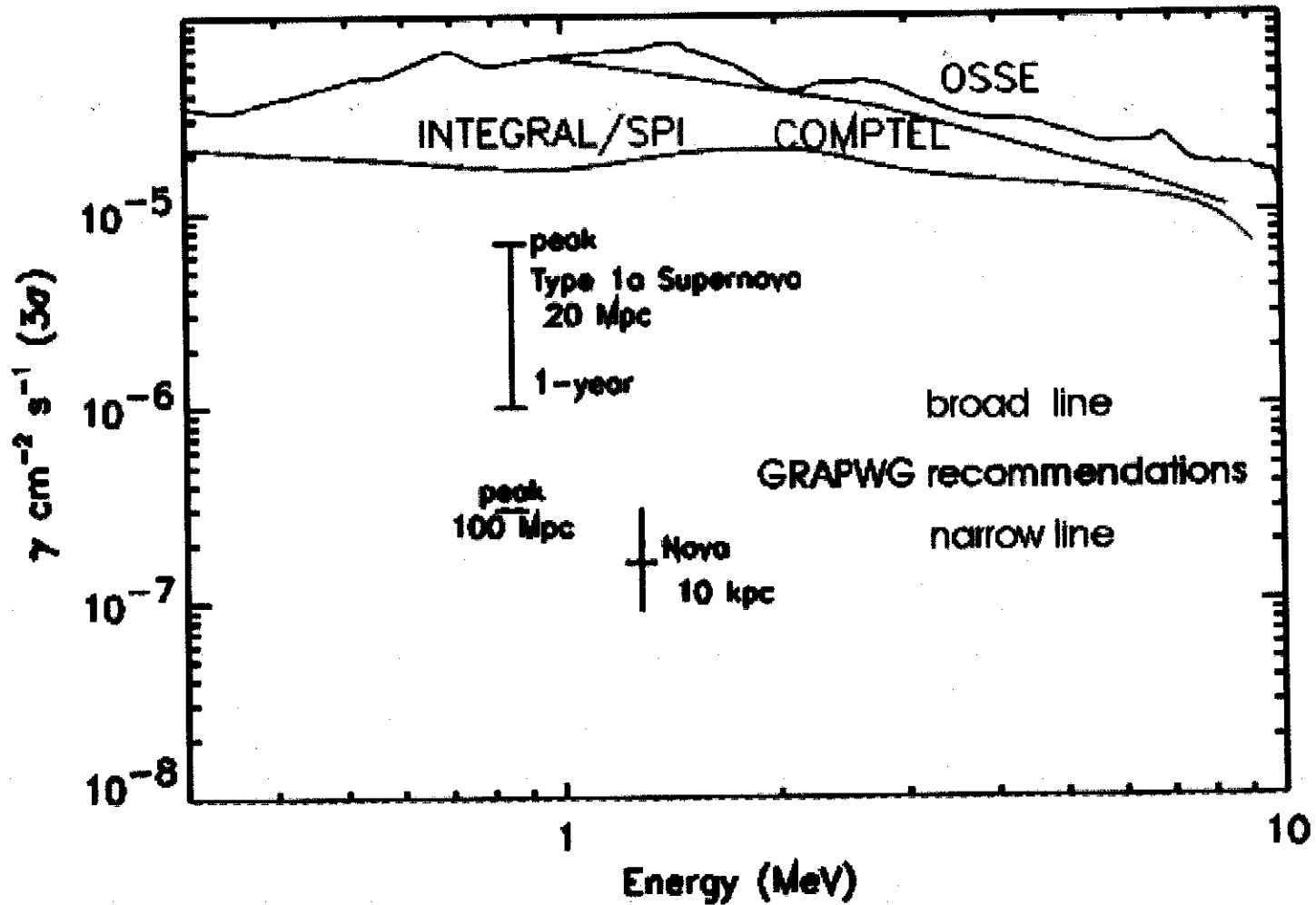
Columbia University

- LXe Properties as Ionization and Scintillation Medium
- Characteristics of the Columbia LXeTPC for MeV Astrophysics
- The Balloon-Borne Liquid Xenon Gamma-Ray Imaging Telescope (LXeGRIT)
- Prospects for a LXe Detector with optimized light and charge readout (CsI photocathodes, Avalanche Photodiodes, GEMs, etc.) for Dark Matter

Advanced Compton Telescope Sensitivity

Sensitivity goal: a factor of > 30 improvement over CGRO and INTEGRAL

- $2 \times 10^{-7} \text{ } \gamma \text{ cm}^{-2} \text{ s}^{-1}$ (3σ) in 10^6 s for narrow lines
- $10^{-6} \text{ } \gamma \text{ cm}^{-2} \text{ s}^{-1}$ (3σ) in 10^6 s for broad lines



Requirements versus Feasibility of a Next Generation Compton Telescope

E. Aprile, A. Curioni, and U. Oberlack (Columbia University)

Goal: A Compton telescope with 3σ line sensitivity of $10^{-7} \gamma \text{cm}^{-2} \text{s}^{-1}$ in 10^6 s observing time. Sensitivity should decrease only by a small factor for line broadening and diffuse emission.

Source detection limit: (with $n\sigma$ significance)

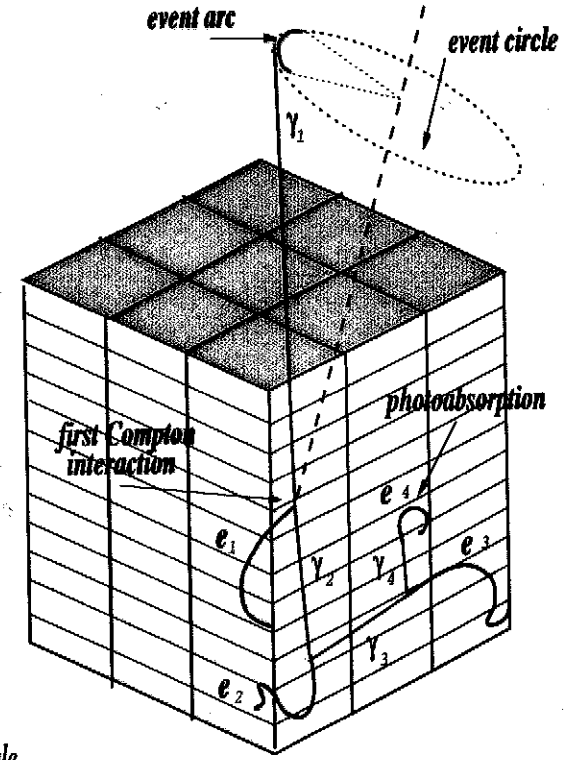
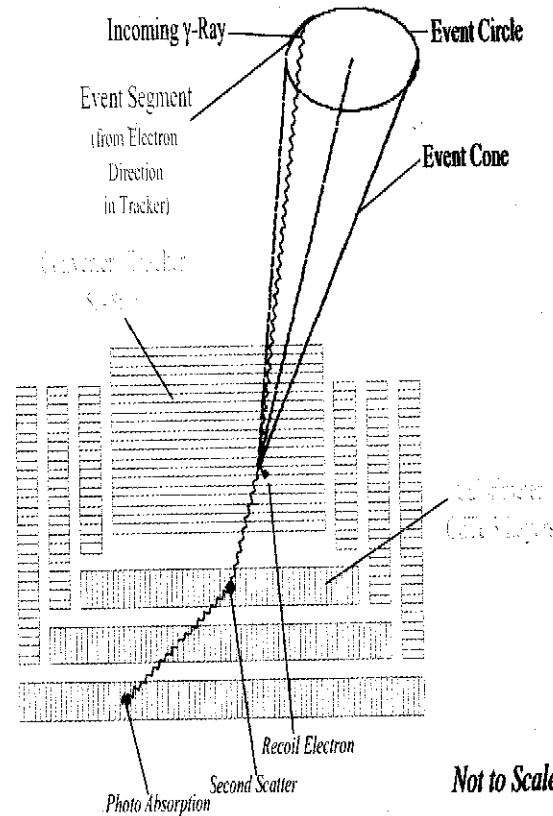
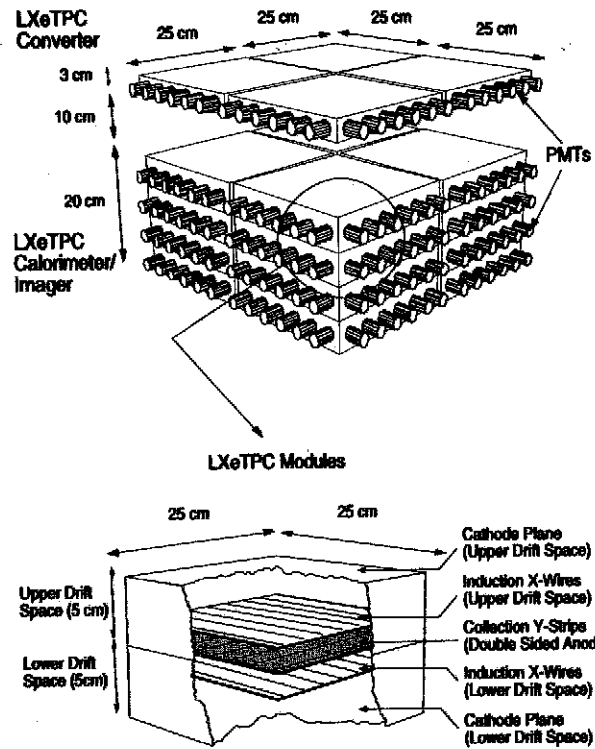
$$f_n = \frac{n^2}{2 A_{\text{eff}} t_{\text{obs}}} \left[1 + \sqrt{1 + \frac{4\alpha f_b A_{\text{eff}} t_{\text{obs}}}{n^2}} \right] \approx n \sqrt{\frac{\alpha f_b}{A_{\text{eff}} t_{\text{obs}}}}$$

$N_b = f_b A_{\text{eff}} t_{\text{obs}}$ is the number of background counts, which defines an "equivalent background flux" f_b . (The approximation holds for dominating background.)

Recipe:

- Increase the effective area by a factor (20–50) in efficiency \times (5–10) in geometrical area = several 100 over COMPTEL.
- Improve background reduction by a factor of ≥ 100 over COMPTEL.
- Use a very large FOV (1/4 – 1/2 of the sky) to increase the observing time for many sources simultaneously. (Additional advantage: Provides a monitor for transient sources à la BATSE for a large fraction of the sky.)

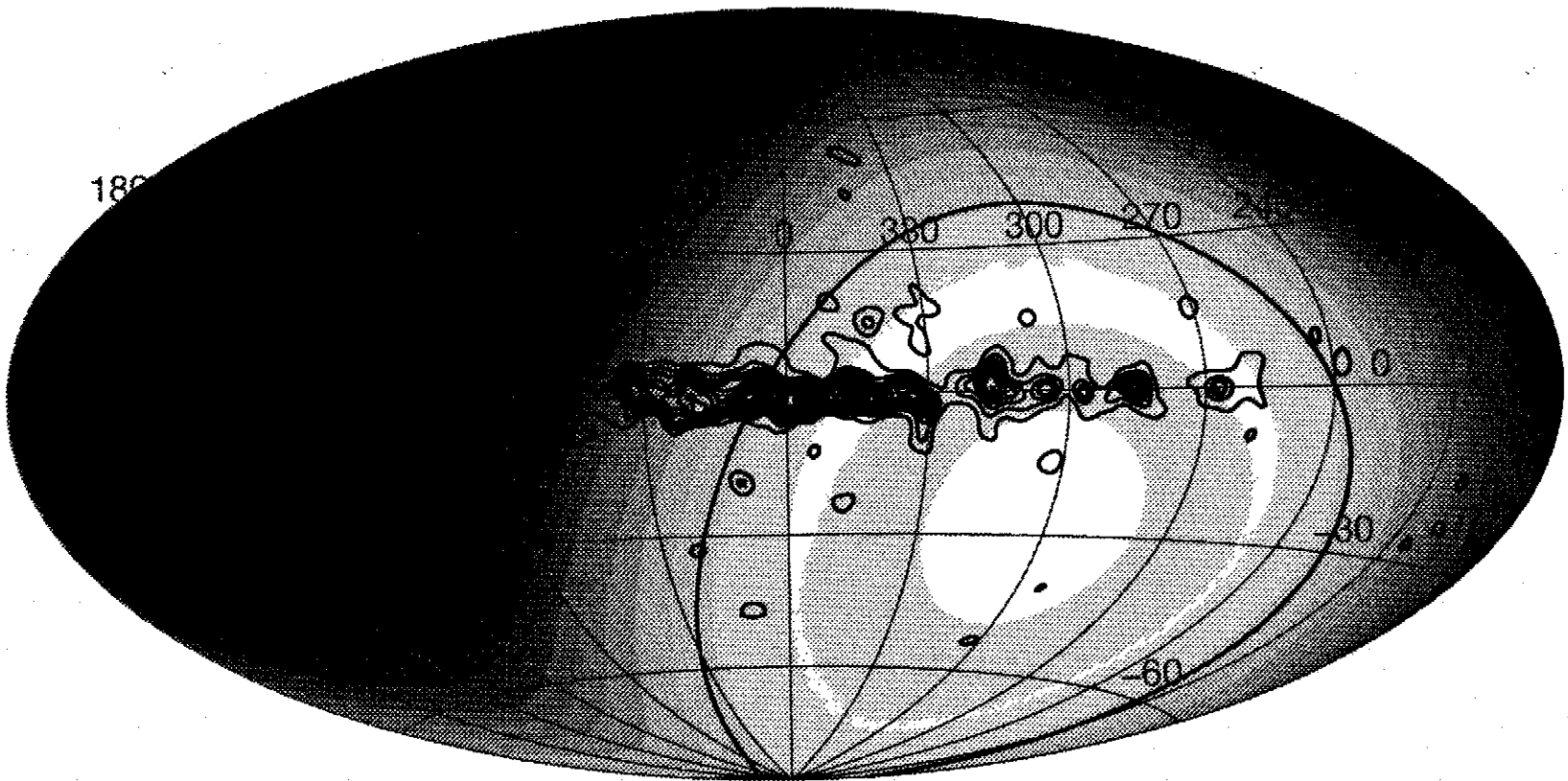
Future Directions for a Compton Telescope at Columbia



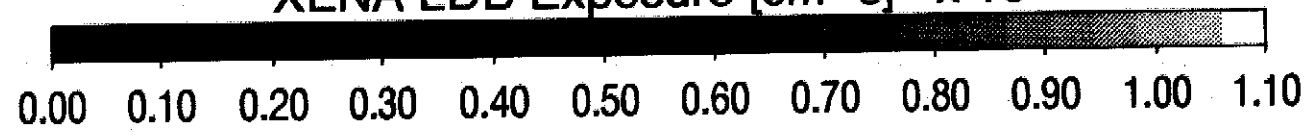
Solid-state Technology

Gas TPC Technology

**LXeTPC Technology Optimized
 from LXeGRIT Design (XENA proposal)**

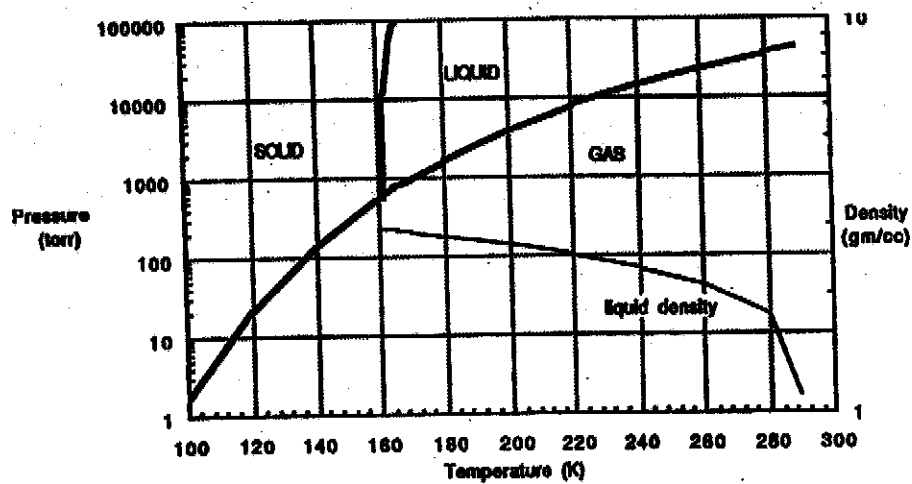


XENA LDB Exposure [cm² s] x 10⁸

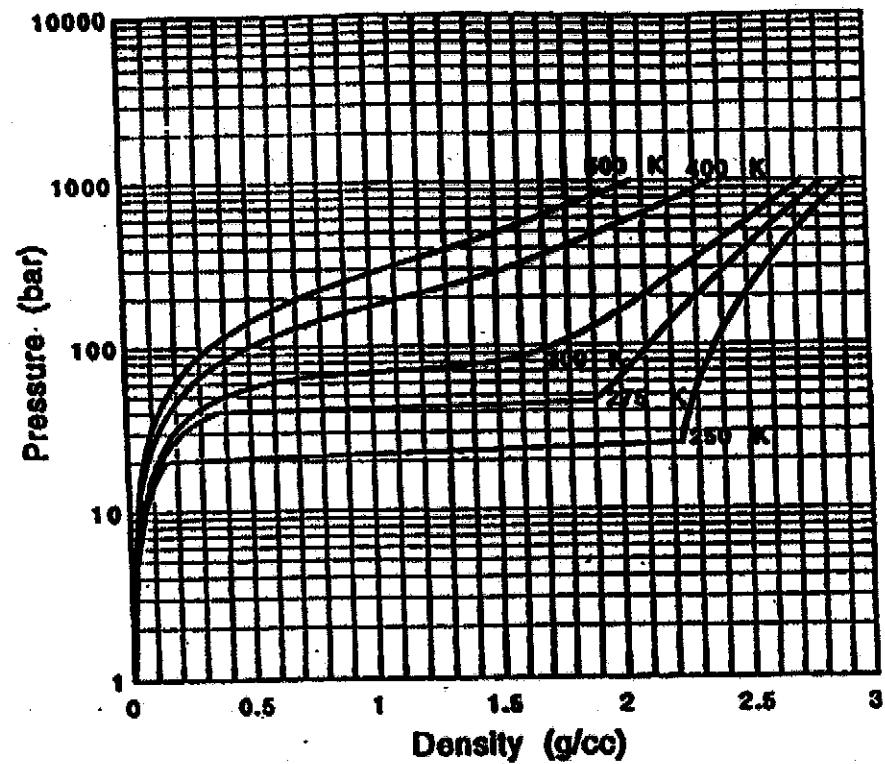


Xenon Phase Diagram

Pressure vs. Temperature



Pressure vs. Density



Liquid Xenon Properties

- High density and atomic number → High stopping power

Material	Density (g/cm ³)	Atomic number	Attenuation length @ 1 MeV (cm)
LXe	3.06	54	5.6
Si	2.33	14	6.7
Ge	5.36	32	3.3

- Small W-value for ionization and scintillation (compared to other gases and liquids)

→ High electron and photon yields

Material	W-value (eV)
LXe	15.6
Other noble gases/liquids	> 20
Si	3.6
Ge	2.8

- Small Fano factor ($F = 0.041$)

→ Excellent energy resolution expected

$$\Delta E/E \propto \sqrt{WF/E_\gamma}$$

$$WF_{\text{LXe}} = 0.64 \text{ eV} \approx WF_{\text{Ge}}$$

- High electron mobility → Fast detector response

$$\vec{v} = \mu \vec{E}$$

Material	Electron mobility μ_e (cm ² V ⁻¹ s ⁻¹)	Mobility of holes (ions) (cm ² V ⁻¹ s ⁻¹)
LXe	4000 @ 195 K	Ion mobility $\mu_i \ll \mu_e$
Si	1900 (21000 @ 77 K)	480 (11000 @ 77 K)
Ge	3800 (40000 @ 77 K)	1800 (40000 @ 77 K)

- Short radiation length and small diffusion constant

→ Good spatial resolution for a TPC

Material	Radiation length X_0 (cm)
LXe	2.8
Si	9.4
Ge	2.3

A Liquid Xenon Imaging Telescope for 1-30 MeV Gamma-Ray Astrophysics

Elena Aprile, Reshmi Mukherjee, and Masayo Suzuki
Columbia Astrophysics Laboratory
Columbia University, New York, NY 10027

ABSTRACT

We discuss the application of a high resolution liquid xenon imaging chamber as a γ -ray telescope for medium energy astrophysics. The chamber, operated in the Time Projection Mode, will be capable to image any ionizing event occurring within its sensitive volume. Gamma-ray events with multiple Compton interactions will be identified as such, thus significantly enhancing the detection efficiency over a wide energy range. This represents the main advantage of the proposed liquid xenon instrument over more conventional double scatter Compton telescopes, in which stringent topological constraints limit considerably the acceptance. In the Compton regime, the excellent energy and position resolution of the detector, on the order of 3% FWHM at 1 MeV and of 250 μm RMS, respectively, will result in a 1σ angular resolution of $0.5^\circ - 0.3^\circ$ for γ -ray energies of 1-20 MeV. The ambiguity in source location that characterizes the Compton measurement can be removed for γ -ray events of high enough energy to allow the reconstruction of the direction of the Compton electron. In the pair production regime, the incoming γ -ray direction can also be uniquely determined from the reconstructed opening angle of the electron-positron pair. An effective discrimination against charged and neutral background events is a direct consequence of the detector imaging capability. The versatility of the liquid xenon telescope and its unique characteristics will allow a large variety of γ -ray emitting sources to be explored with high sensitivity.

1. INTRODUCTION

Observations of the gamma-ray sky in the low and medium energy range below about 30 MeV promise to provide a wealth of information on the nature of the source or region in which the gamma-rays are produced. The difficult experimental problems encountered in this energy region have resulted in a slower development than in other regions of the electromagnetic spectrum. Even though considerable progress has been achieved during the last few years and a wealth of new information is expected from the four instruments planned for the Gamma Ray Observatory (GRO) mission, it is clear that improved experimental techniques are needed for future gamma-ray observations. The application of rare gas liquids, such as xenon, promise major advances in detector efficiency, imaging and background reduction capabilities as well as detector energy and spatial resolution.

Among the properties which make a liquid xenon imaging chamber especially suited for gamma-ray astronomy are:

1. High detection efficiency due to the high density ($\rho = 3.06 \text{ g/cm}^3$) and high atomic number ($Z = 54$).
2. Excellent energy resolution, ultimately similar to that of germanium.
3. Excellent spatial resolution, ultimately a few tens of μm .
4. Excellent scintillation efficiency, comparable to that of NaI(Tl) and with a fast component, ideal for event triggering.
5. Three-dimensional track reconstruction which allows bubble chamber like images of multiple gamma-ray interactions.
6. Excellent background rejection capability due to track imaging and to pulse shape discrimination of the scintillation signal.
7. Short radiation length ($L_{\text{rad}} = 2.6 \text{ cm}$), ideal for a compact calorimeter.

$$Q(t) = Q_0 \frac{\tau}{t} [1 - e^{-t/\tau}]$$

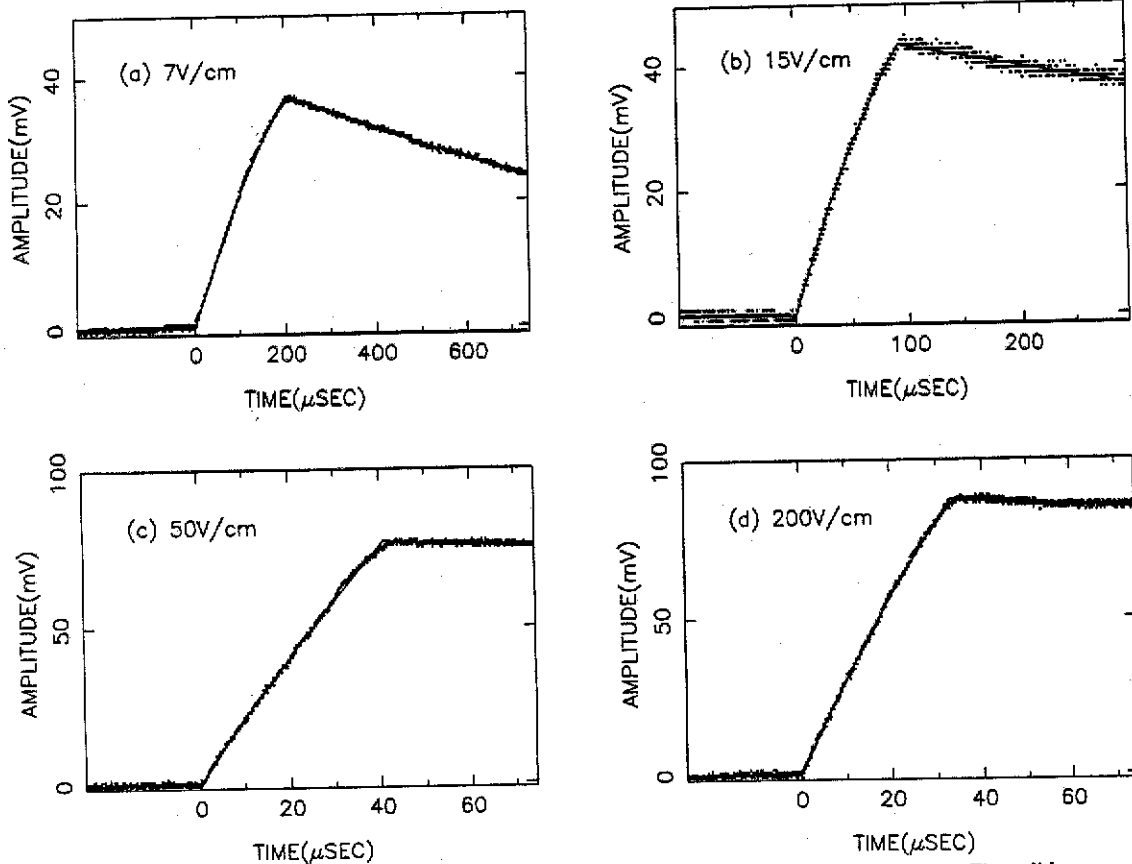


Fig. 3. Typical ionization signals generated by cosmic ray tracks in liquid xenon at different electric fields. The solid curves are the result of the fit with the theoretical pulse shapes.

time. In our data this is true down to the lowest field. The results for the electron drift velocity in liquid xenon at 195 K are shown in fig. 5 as a function of the applied electric field. The error bars include an overall systematic uncertainty of approximately 10%. For comparison, data obtained at 200 K and 163 K by Gushchin

et al. [23] and at 216 K and 165 K by Huang and Freeman [24] are shown on the same figure. Our points at 195 K clearly lie in between the other data, and show

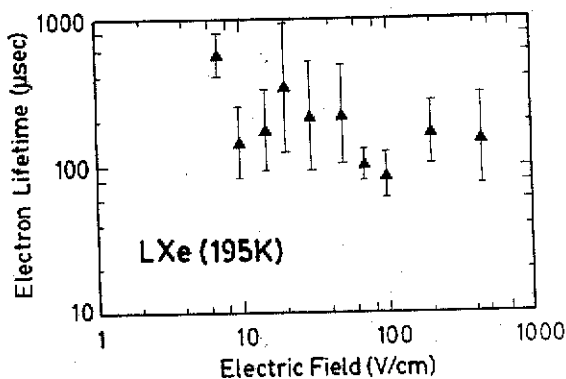


Fig. 4. Electric field dependence of the average electron lifetime in liquid xenon at $T = 195$ K.

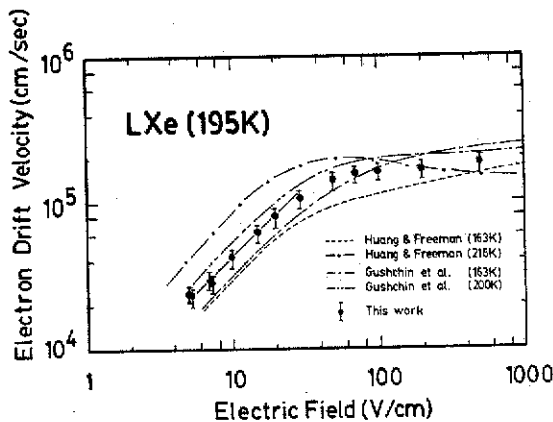


Fig. 5. Electric field dependence of the electron drift velocity in liquid xenon at $T = 195$ K. The solid line is the fit of $v_d = \mu_0 E$, giving $\mu_0 = (4230 \pm 400) \text{ cm}^2 \text{ V}^{-1} \text{ s}^{-1}$. Other lines are from refs. [23,24].

$$\bar{\tau}_{\text{LXe}} \approx 200 \mu\text{sec}$$

$$\bar{\tau} = \frac{1}{k_S [S]} = \frac{1}{k_S \cdot p \cdot n_{\text{Xe}}} \Rightarrow p \leq 0.3 \text{ ppb } O_2 \text{ equivalent}$$

$$\lambda = \bar{\tau} v_d \approx 40 \text{ cm}$$

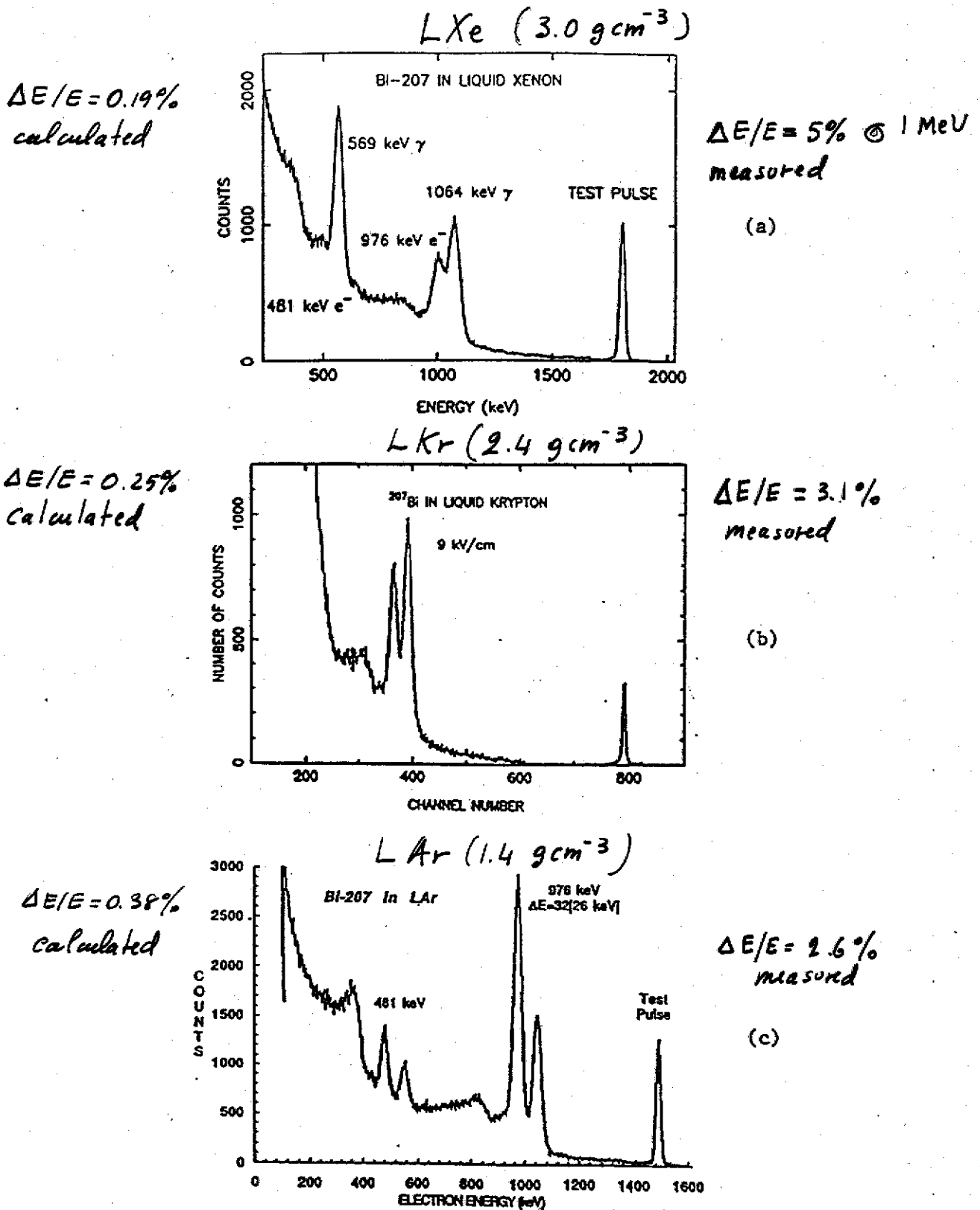


Fig. 2 ^{207}Bi spectra (a) in LXe at 12 kV/cm [ref. 7]; (b) in LKr at 9 kV/cm [ref. 10]; and (c) in LAr at 11 kV/cm [ref. 9].

Mechanism(s) for Energy Resolution deviation from Fano limit must be density dependent

XENON SCINTILLATION

$$\lambda = 1750 \text{ \AA}$$

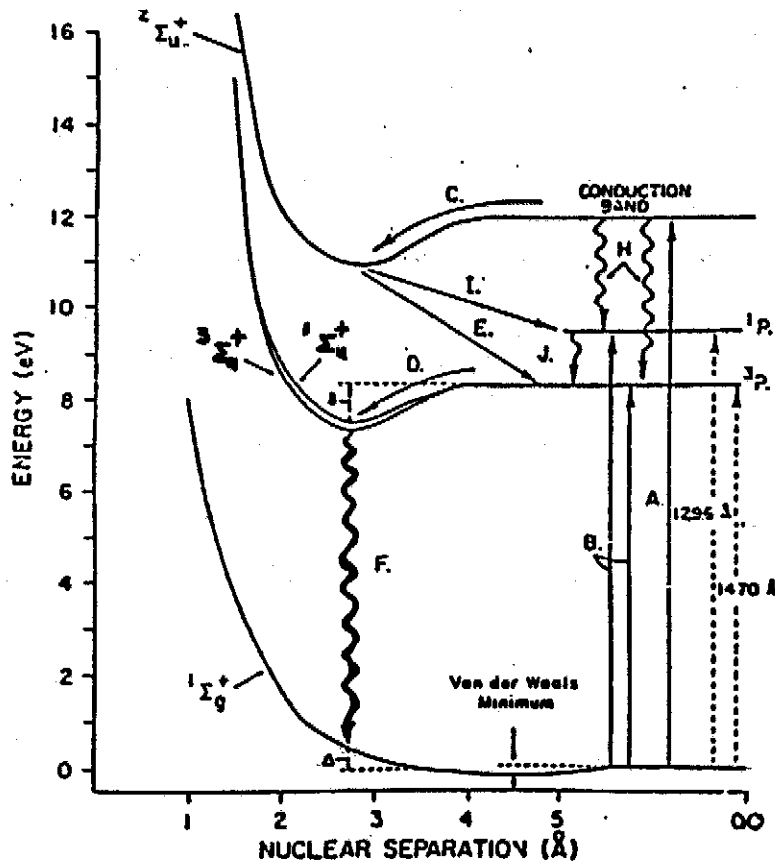
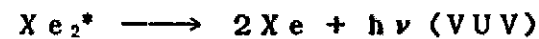
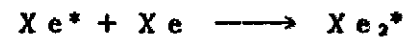
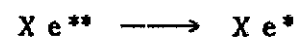
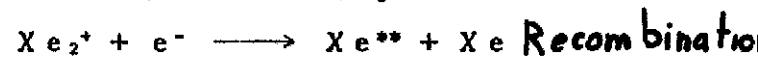
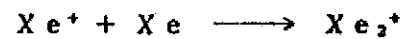
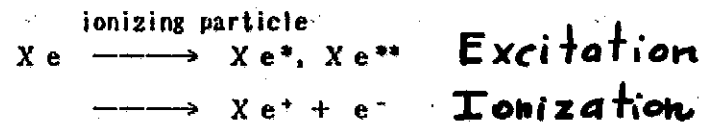
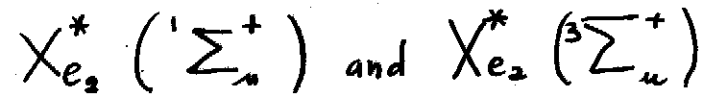


FIG. 4. Schematic energy diagram of xenon with some atomic and molecular transitions. ${}^2\Sigma_u^+$ is the ionic core state, ${}^{1,3}\Sigma_u^+$ are the lowest excited states of the Xe_2^+ excimer, and ${}^1\Sigma_g^+$ is the excimer's repulsive ground state. Luminescent and non-luminescent transitions are wavy and straight lines, respectively. Transitions A through J are described in the text. The molecular dissociation energy is δ and the repulsive ground-state energy is Δ . The van der Waals minimum at about 4.5 \AA is exaggerated.



Radiative de-excitation of



Fast
 $\tau_1 = 3 \text{ ns}$

Slow
 $\tau_2 = 27 \text{ ns}$

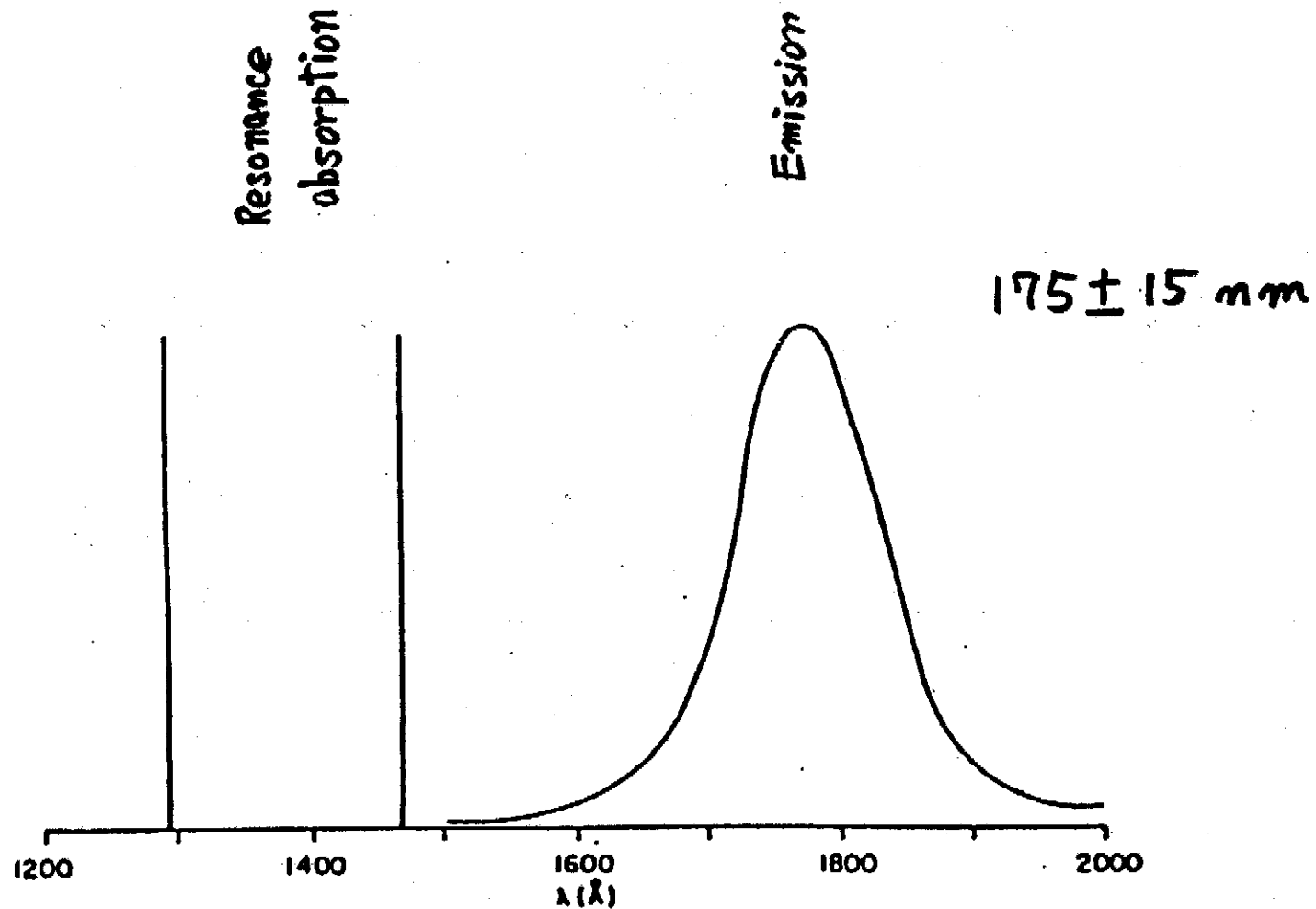
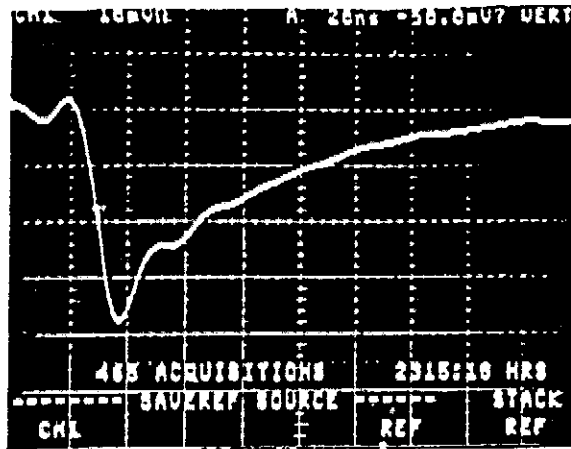


FIG. 3. LXe emission spectrum from alpha particle excitation. The broad excimer emission band is shown relative to the two atomic resonance absorption lines. The amplitude relationships are arbitrary.

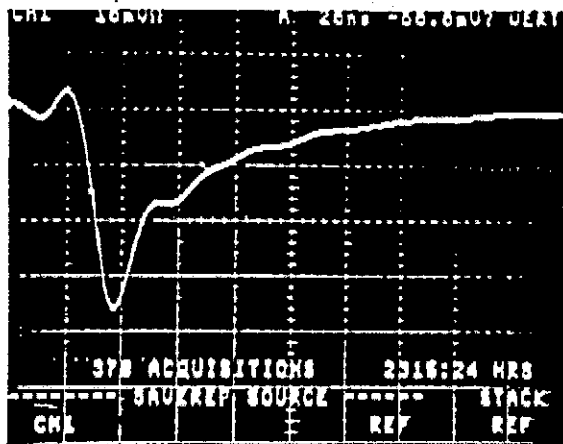
TIME DEPENDENCE OF LXe SCINTILLATION

ELECTRONS



(a) $\vec{E} = 0$

slow recombination
light superimposed
on excitation
light

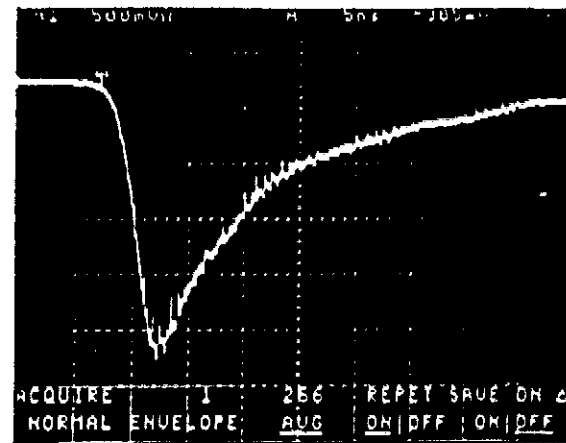


(b) $\vec{E} = 2 \text{ kVcm}^{-1}$

Figure 2. Scintillation light of ^{207}Bi conversion electrons in liquid xenon (a) without and (b) with an applied electric field of 2 kV/cm (10 mV/div., 20 nsec/div.).

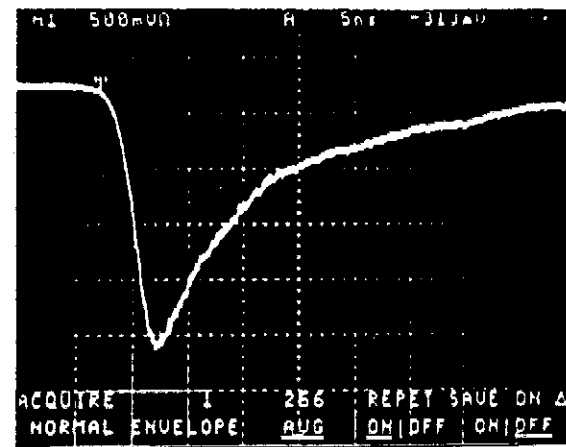
Recombination Process for e^-
is slow

ALPHA PARTICLES



(a) $\vec{E} = 0$

fast component
enhanced



(b) $\vec{E} = 7.9 \text{ kVcm}^{-1}$

Figure 3. Scintillation light of ^{241}Am alpha particles in liquid xenon (a) without and (b) with an applied electric field of 7.9 kV/cm (500 mV/div., 5 nsec/div.).

Recombination Process for α
is fast

Aprile et al. 1989

Time dependence
of Liq. Xe scintillation

For minimum ionizing particles,

$$i(t) = i_1 + i_2 + i_r = A_1 \cdot \exp(-t/\tau_1) + A_2 \cdot \exp(-t/\tau_2) + A_r \cdot \exp(-t/\tau_r)$$

$i_1(t)$: decay from a singlet state of Xe_2^* (fast)

$i_2(t)$: decay from a triplet state of Xe_2^* (slow)

$i_r(t)$: recombination of ions and electrons

$$I(t) = \int_0^t i(t) dt = I_1(t) + I_2(t) + I_r(t)$$

$$= A_1 \tau_1 (1 - \exp(-t/\tau_1)) + A_2 \tau_2 (1 - \exp(-t/\tau_2)) + A_r \tau_r (1 - \exp(-t/\tau_r))$$

$$I(\infty) = A_1 \tau_1 + A_2 \tau_2 + A_r \tau_r$$

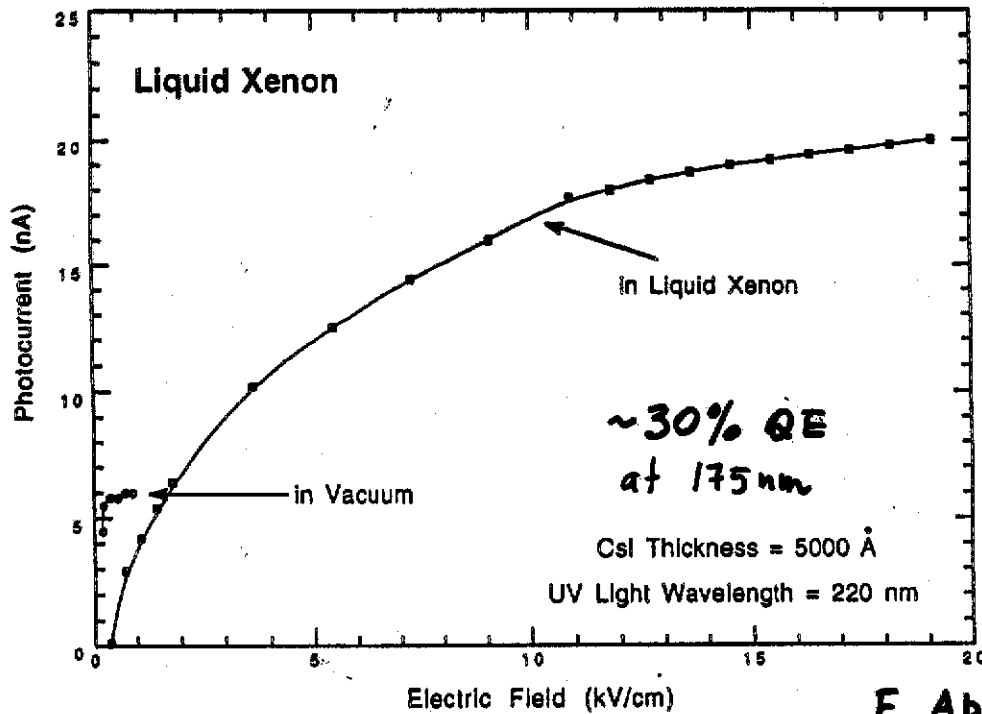
$$\tau_1 = 2.2 \text{ ns}, \quad \tau_2 = 27 \text{ ns}, \quad \tau_r = 45 \text{ ns}$$

$$A_1/A_2 = 0.6, \quad (A_1 \tau_1 + A_2 \tau_2)/I(\infty) = 0.26$$

$$\Rightarrow A_1 = 0.0055, \quad A_2 = 0.0092, \quad A_r = 0.0164$$

$$(I(\infty) = 1, \quad \tau \text{ in ns})$$

First Observation of Liquid Xenon Scintillation with a CsI photocathode



E. Aprile et al.
NIMA 343 (1994)

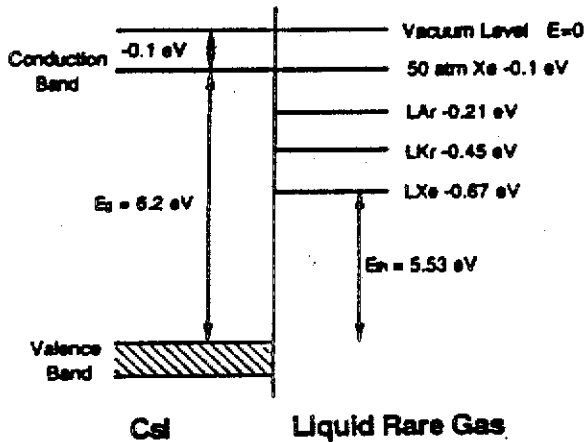


Fig. 8. Band structure at the CsI-liquid interface.

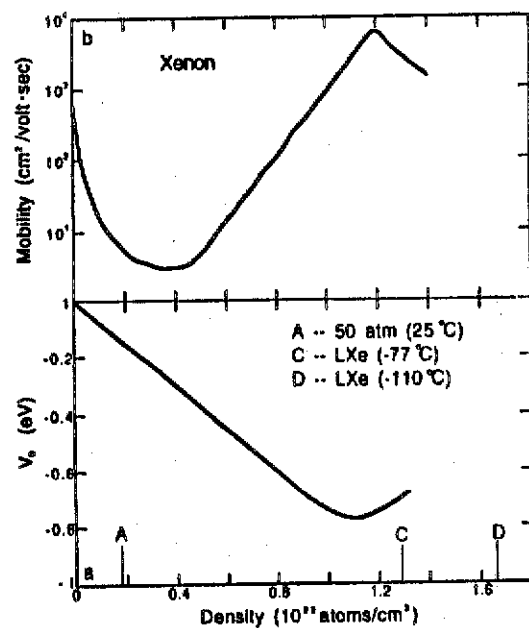


Fig. 9. (a) V_0 and (b) the zero-field electron mobility as a function of Xe density [31].

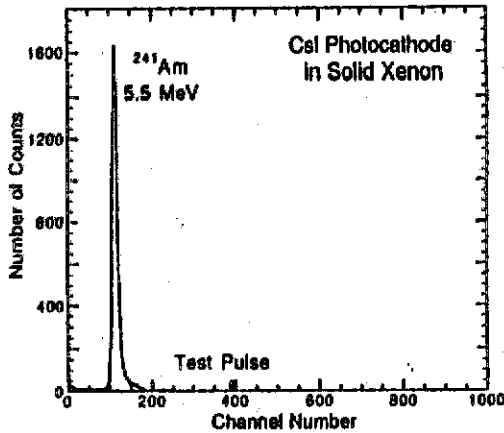


Fig. 2. Typical pulse height spectrum of the scintillation light from ^{241}Am 5.5 MeV α -particles in solid Xe.

due to the lower vapor pressure, high voltage breakdown occurred earlier than in the liquid phase. This prevented us from reaching high electric fields.

4. Results

The data in solid Xe were obtained with the 500 nm thick CsI photocathode. Fig. 2 shows a typical pulse height spectrum of the scintillation light produced in solid Xe by the alpha particles. Compared to the same data measured in the liquid phase at the same electric field and electronics gain, the peak position is higher. Results obtained in different runs made with liquid and solid Xe are summarized in Fig. 3. One can see that the results obtained with liquid Xe are reproducible in the different runs and in good agreement with our previous results [3]. In the case of the solid, results are different depending on the procedure

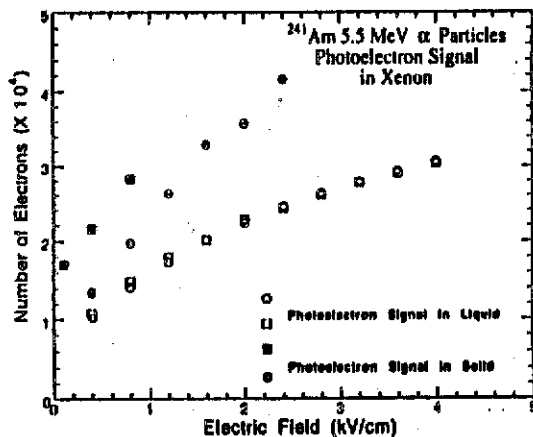


Fig. 3. Number of electrons collected as a function of the electric field from the CsI photocathode for 5.5 MeV ^{241}Am alpha particles in liquid and solid Xe.

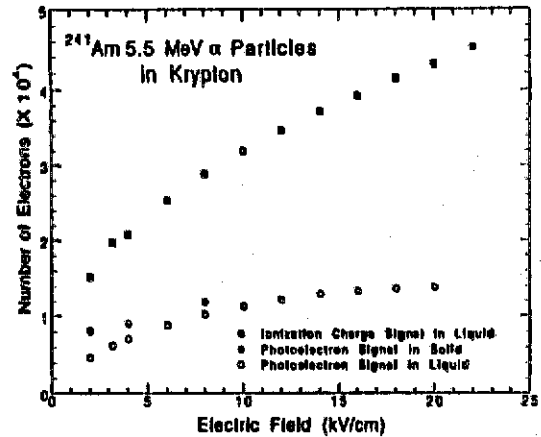


Fig. 4. Number of electrons collected as a function of the electric field from the CsI photocathode for 5.5 MeV ^{241}Am alpha particles in liquid and solid Kr.

followed to form the solid. For a given solid sample the results were stable with time with a fluctuation less than a few percent. The light signal from solid Xe was highest (closed squares in Fig. 3) when we condensed the xenon gas into solid with a LN_2 bath. If the Xe gas was first condensed into liquid with a bath of alcohol and LN_2 mixture (about -110°C), then cooled down to form solid by changing the bath to LN_2 , the observed light signal was lower (closed circles in Fig. 3). Despite the variation in the data from different solidification procedures, the measured light signal was however always a factor of 50-100% higher than that measured in the liquid phase. The variation in the measured photoelectron signal is related to the quality of the solid. In our experiments, the solid structure was always polycrystalline and in some cases with many defects.

The energy resolution for the light produced by the alpha particles in solid Xe at the maximum applied electric field of 2 kV/cm, was typically 10-12%, dominated by

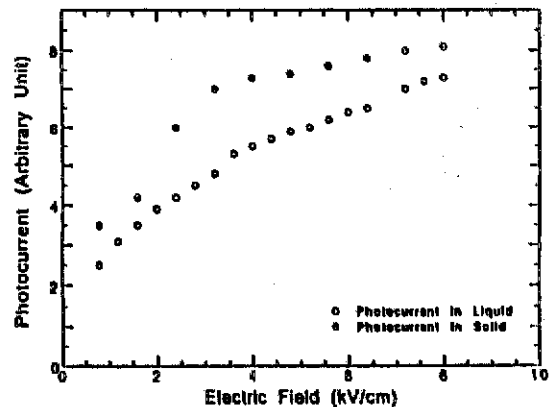
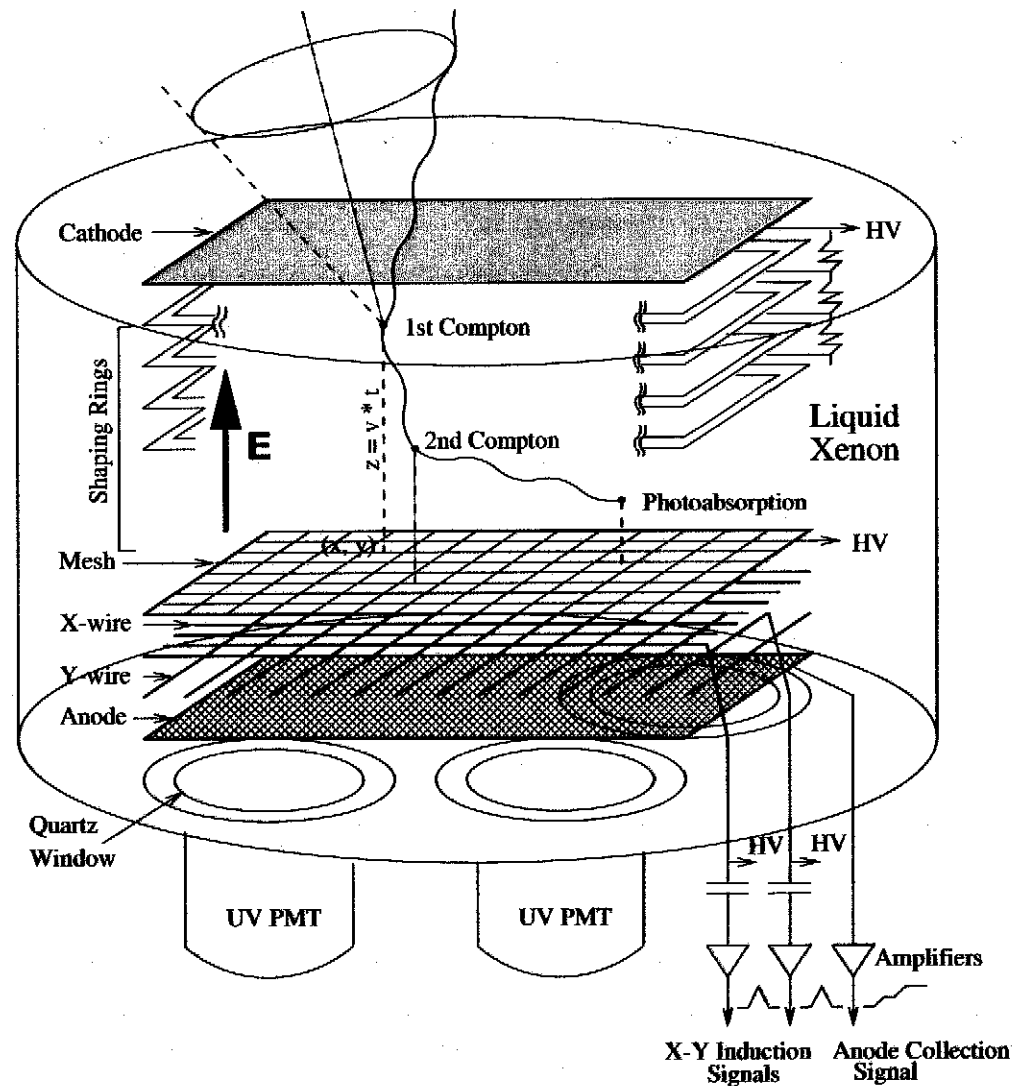


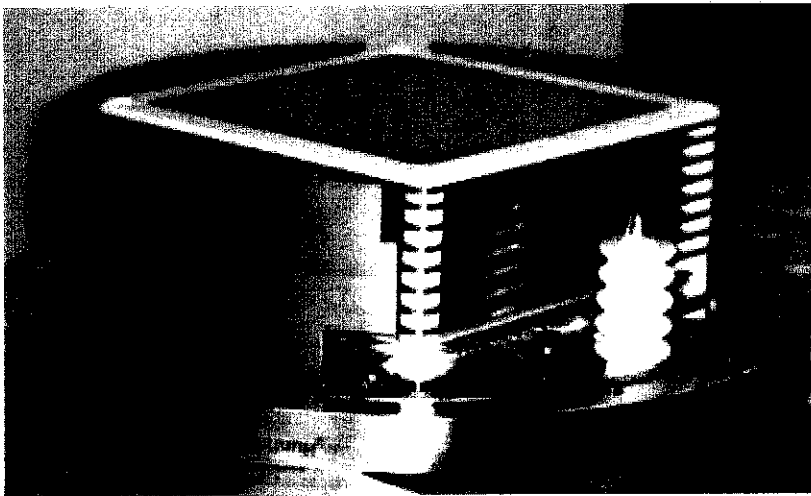
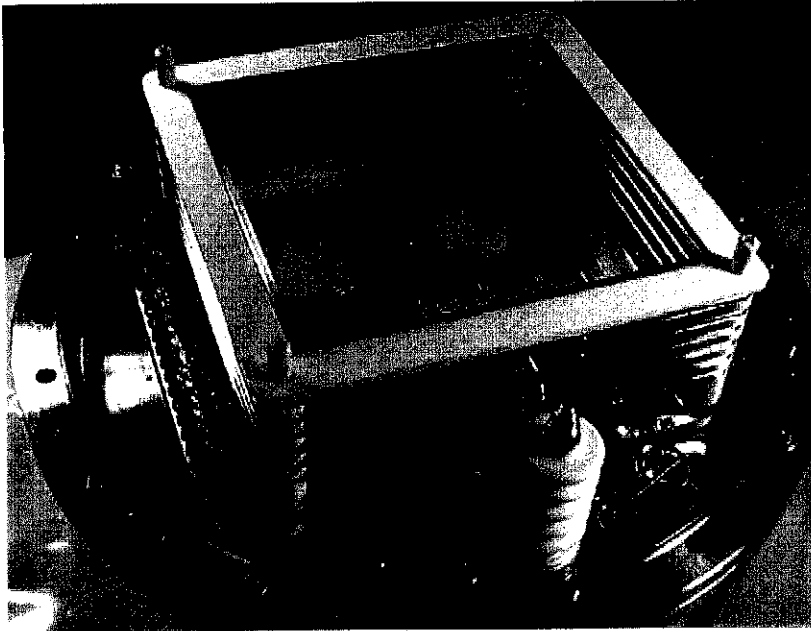
Fig. 5. Photocurrent from the CsI photocathode in liquid and solid Kr for experiments using the mercury lamp.

The Liquid Xenon Time Projection Chamber as Compton Telescope

- A homogeneous, self-triggered detector which combines high detection efficiency with calorimetry and 3D event imaging
- Xe ionization and scintillation detected to measure energy and spatial information for each gamma-ray interaction in the sensitive volume
- Events with multiple interactions are identified and used for reconstructing the incoming gamma-ray energy and direction, with Compton kinematics
- Events with a single interaction and high energy charged particles easily rejected. Background is reduced with 3D event imaging

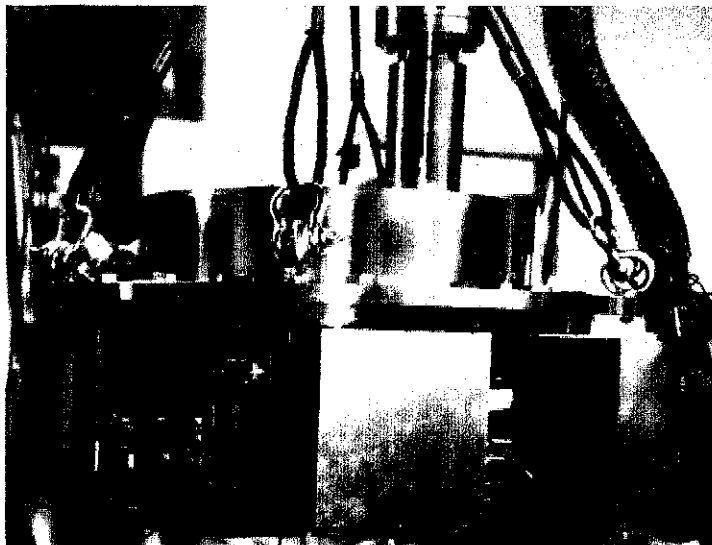
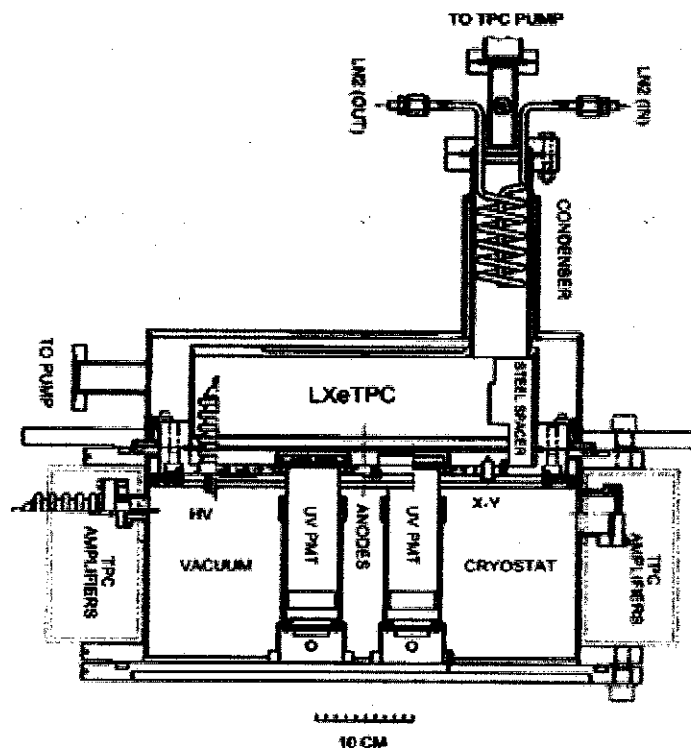
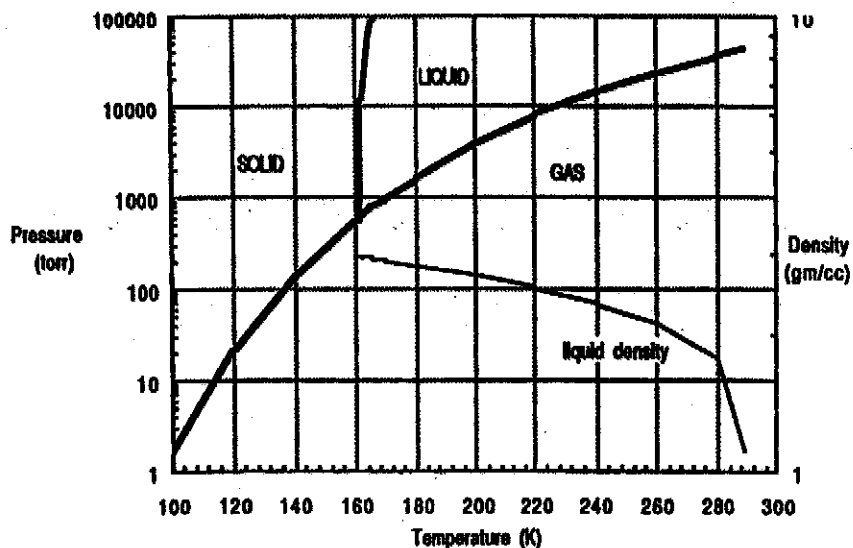


The Liquid Xenon Time Projection Chamber Developed at Columbia



- 24 kg active Xe mass.
- 20×20 cm² active area
- 7 cm drift gap (21 gcm⁻²)
- 1 kV/cm electric field
- 4 UV PMTs for Xe scintillation light.
- 62+62, 100 μm, 3 mm pitch wires for X-Y localization.
- 4 independent anodes for total energy measurement.
- 1 mm X-Y spatial resolution from digitized wire signals.
- 300 μm Z spatial resolution from absolute drift time measurements (max=35 μs)
- 8.8% FWHM energy resolution at 1 MeV from digitized anode signal(s).
- "Inactive" LXe reduced with SS spacers.

The Liquid Xenon Time Projection Chamber Cryostat

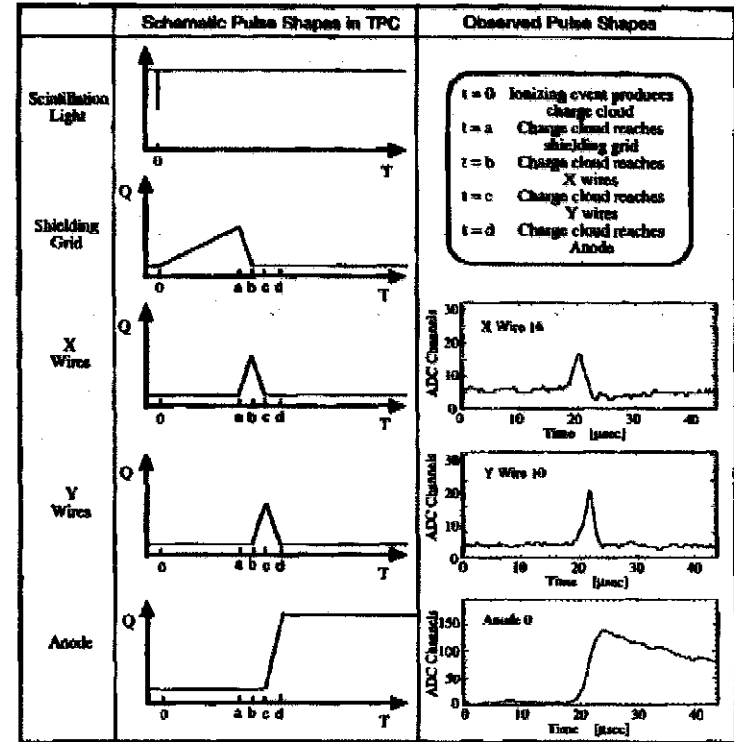


- LXeTPC insulated by a vacuum cryostat 50 cm diameter and 35 cm high).
- Cathode HV supply and filter, PMTs and wires HV decoupling inside cryostat.
- Xe gas condensed and kept at desired temperature by a controlled flow of LN₂ through a copper coil.
- Vapor pressure and thus LXe temperature allowed to vary between 1.5 atm (-95°) and 2.4 atm (-91°). Flight Dewar (90 l LN₂) hold time is about 40 hours.

LXeTPC Signal Formation and Read-Out

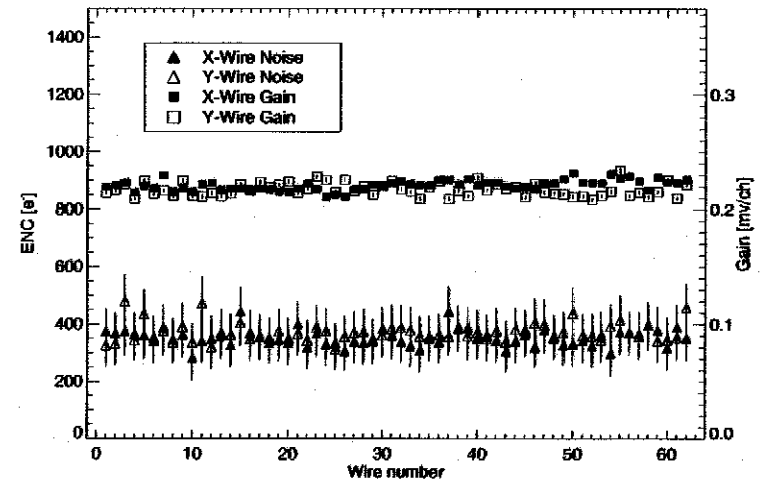
Charge Signal

- Charge produced in liquid xenon per 100 keV energy deposit:
 $N_e = 100 \text{ keV} / 15.6 \text{ eV} \sim 6,400 e^-$
- Electrical field adapted to focus electrons through holes of grid and through the wire spacing
- Induction signal from drifting charge on the wires
- $\sim 75\%$ of the charge is collected on the anodes at a field of 1 kV/cm
- Signals on wires and anodes are digitized by 5 MHz flash ADCs with 8 bit and 10 bit precision, respectively



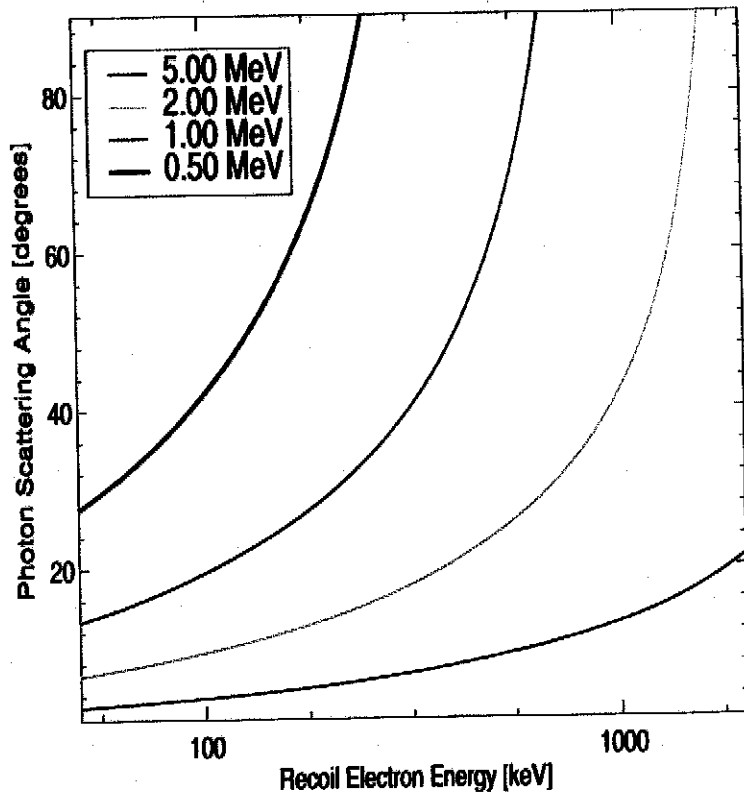
Electronics Noise

- Low noise conditions required for 3-dimensional imaging of MeV γ -rays, which interact in multiple points within the detector.
- Electronics noise level in LXeGRIT in units of equivalent noise charge (ENC):
 Wires: $\sim 350 e$
 Anodes: $\sim 850 e$ (higher capacitance).

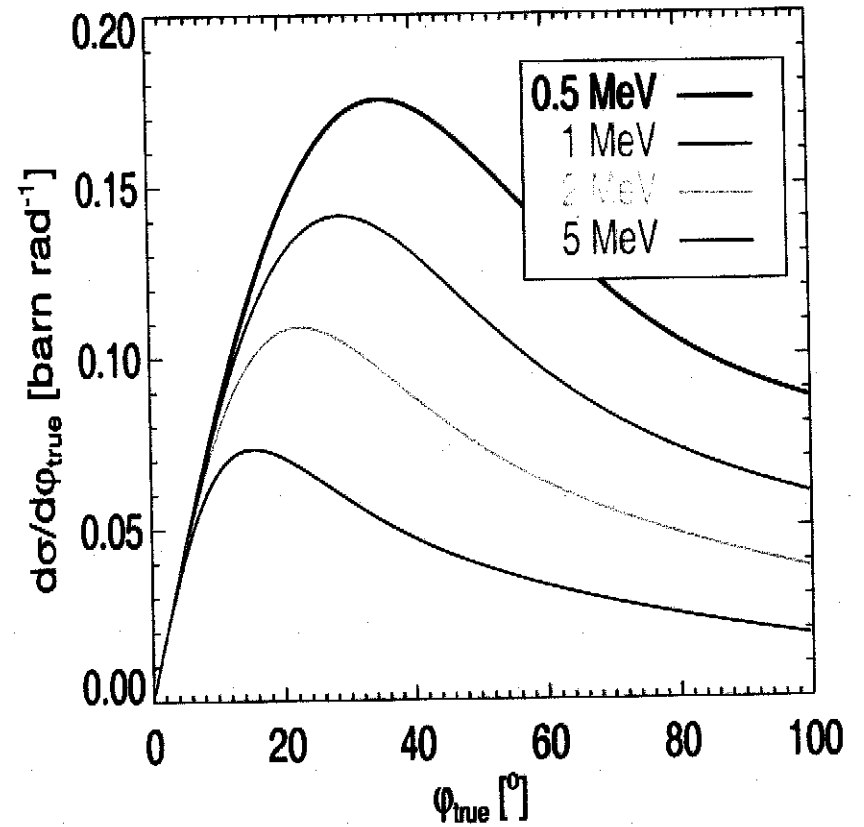


Compton Scattering Kinematics

Photon Scattering Angle vs. Recoil Electron Energy



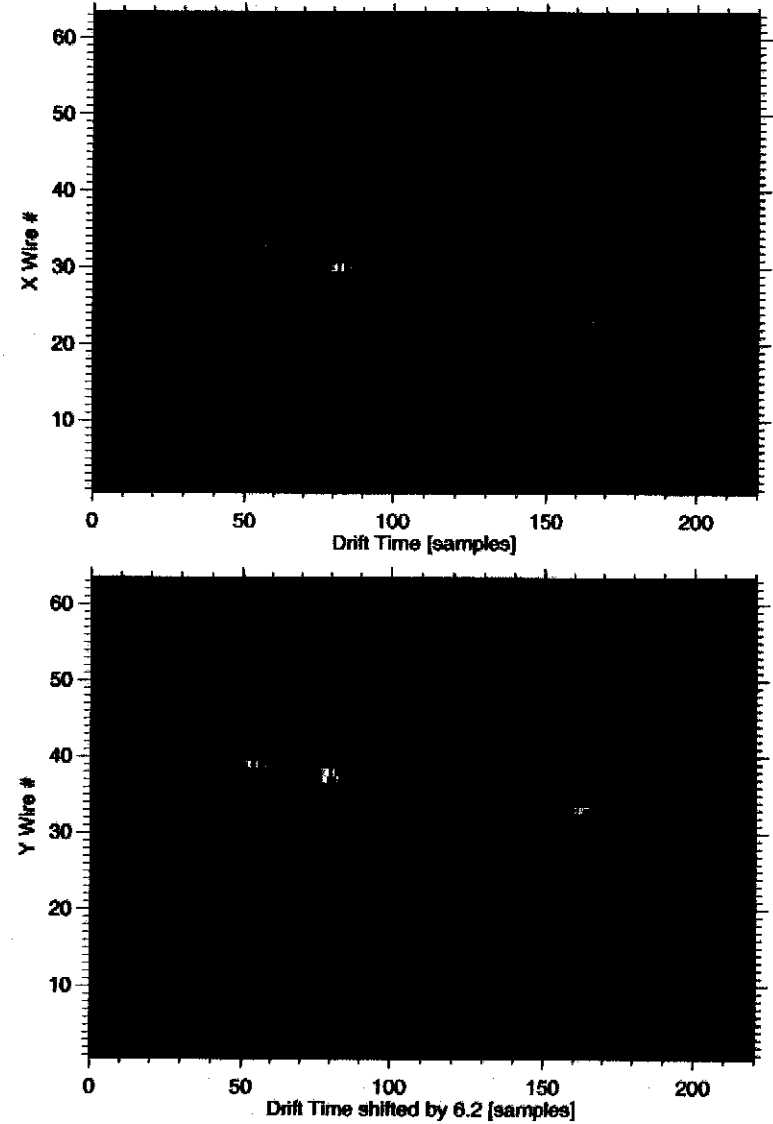
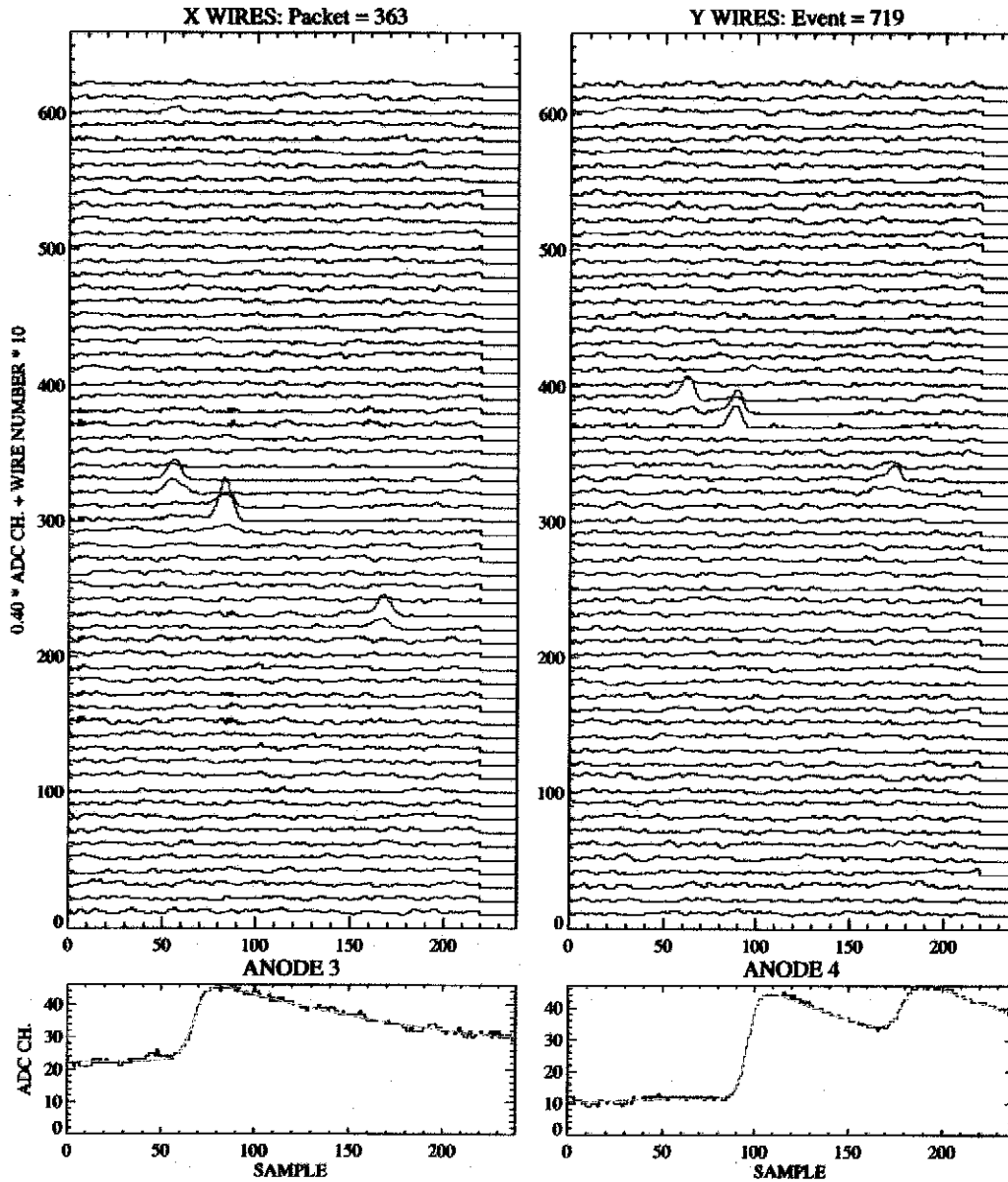
Cross Section vs. Photon Scattering Angle



Signal Recognition and Event Reconstruction

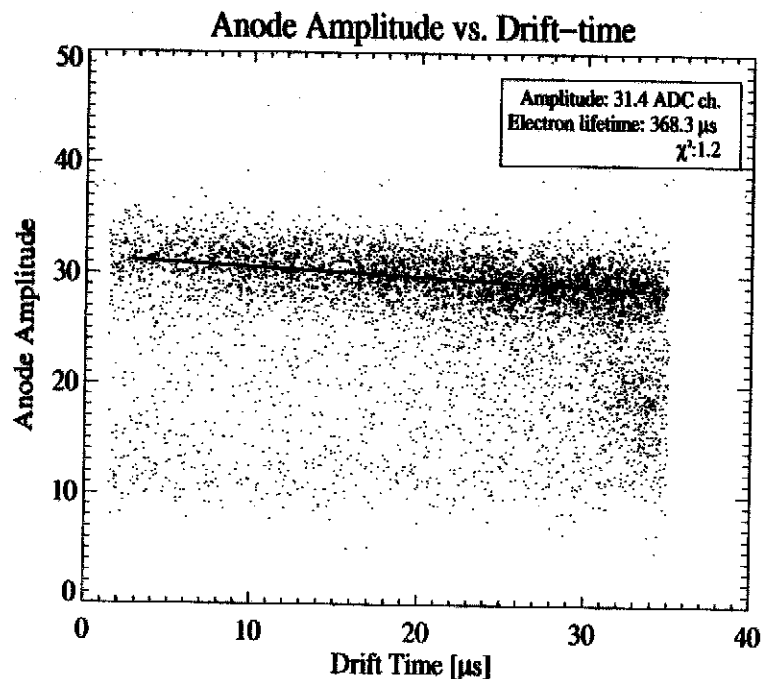
X-/Y-Wire and Anode Signals vs. Drifttime
 γ -ray with three interactions in the detector.

False Color Display of X-/Y-Wire Signals
(same event)

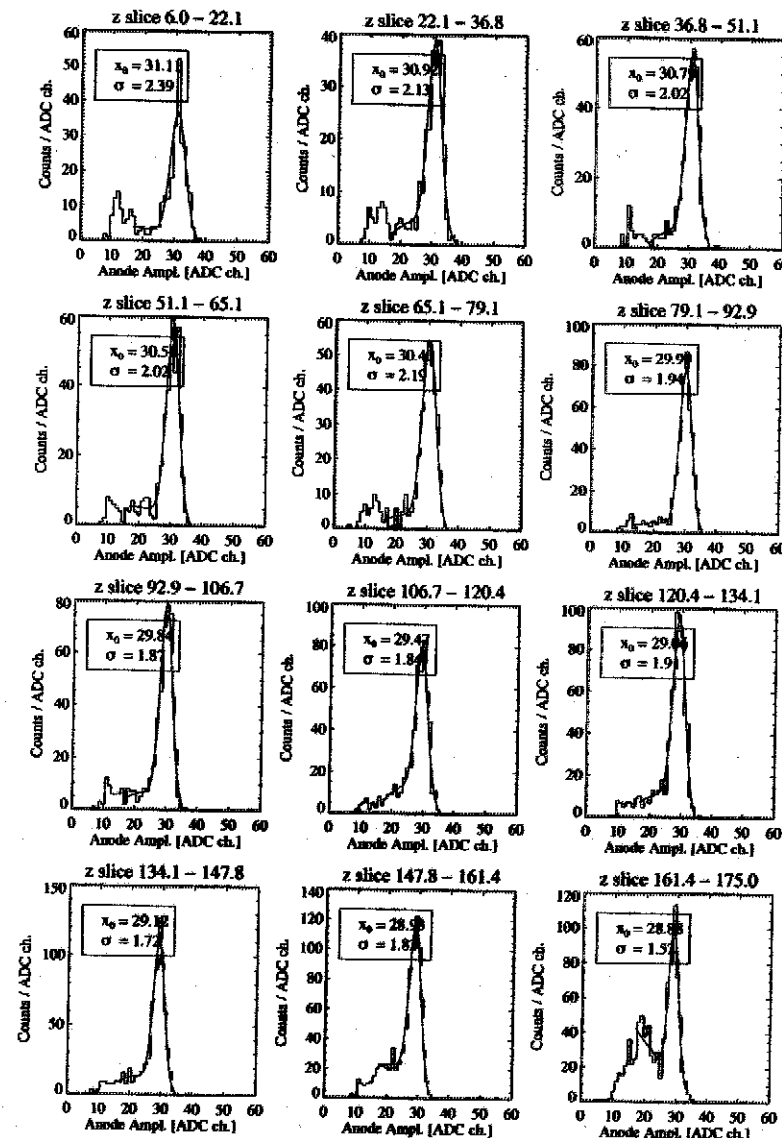


Liquid Xenon: the purity level inferred from ^{137}Cs γ -rays data

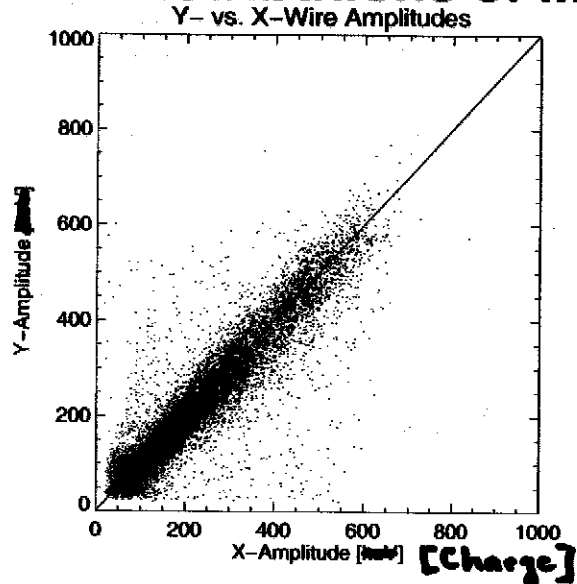
energy spectra for different (increasing) drift lengths



- Measured z-coordinates yield a measurement of the electron attachment (charge loss) as a function of drift distance
- Lifetime of a drifting electron: typically $400 \mu\text{s}$
- Signal amplitudes are corrected for charge loss according to their z-location
 \Rightarrow improved spectral performance

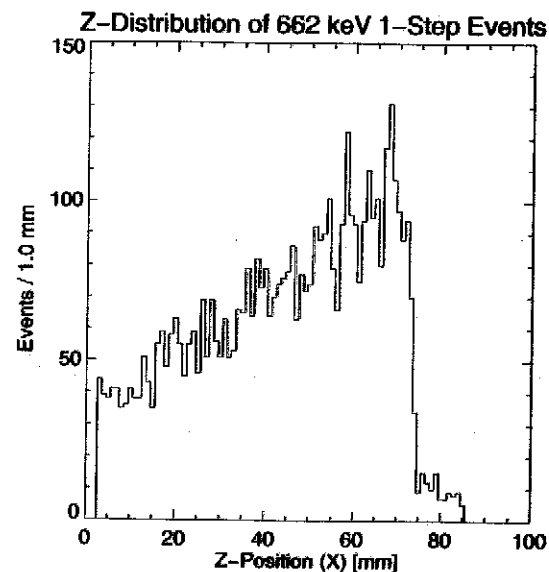
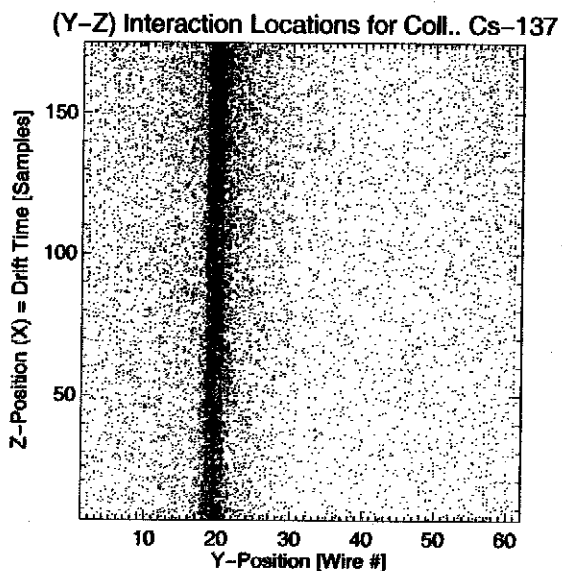
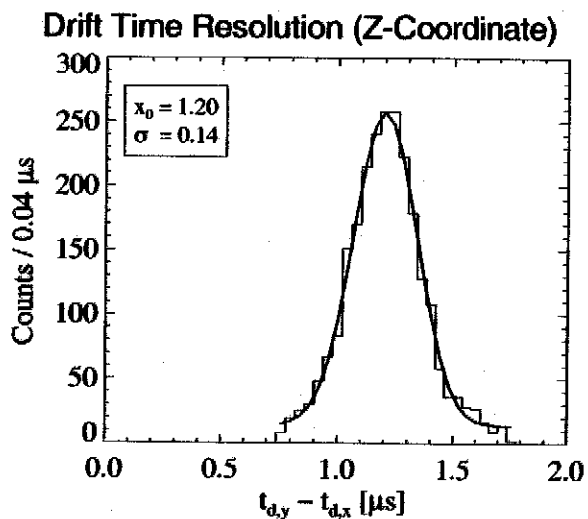
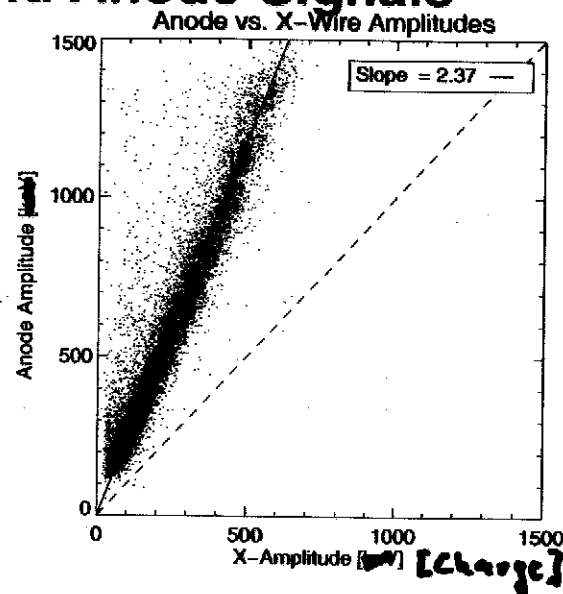


Distributions of Matched X-Wire, Y-Wire, and Anode Signals



Top row: Close correlation of charge measured on matching X-Y-wire signals and on the corresponding anode confirms successful signal recognition.

Bottom row: Imaging a collimated Cs-137 beam with the LXeTPC.



From Laboratory Prototype to Balloon-Borne Instrument

The Liquid Xenon Gamma-Ray Imaging Telescope Collaboration

*E. Aprile¹, A. Curioni¹, K. L. Giboni¹, M. Kobayashi¹, U. Oberlack¹, C Zhang¹,
S. Ventura^{1,2},
T. Doke³, J. Kikuchi³,
E. L. Chupp⁴, P. P. Dunphy⁴*

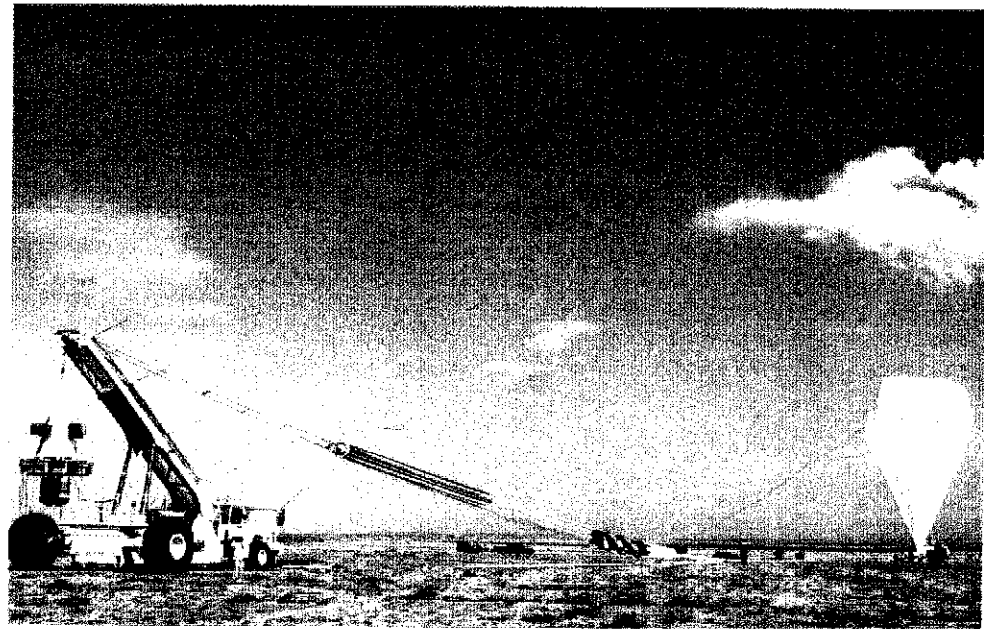
¹Columbia University, New York, USA

²INFN / University of Padua, Italy

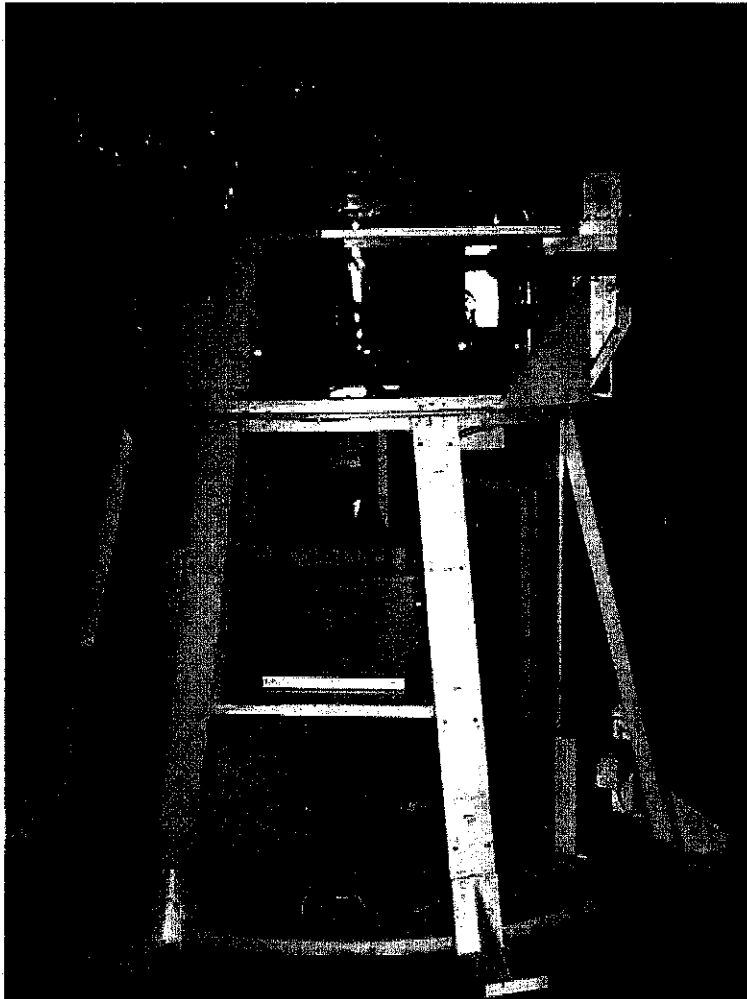
³Waseda University, Japan

⁴University of New Hampshire, Durham, NH, USA

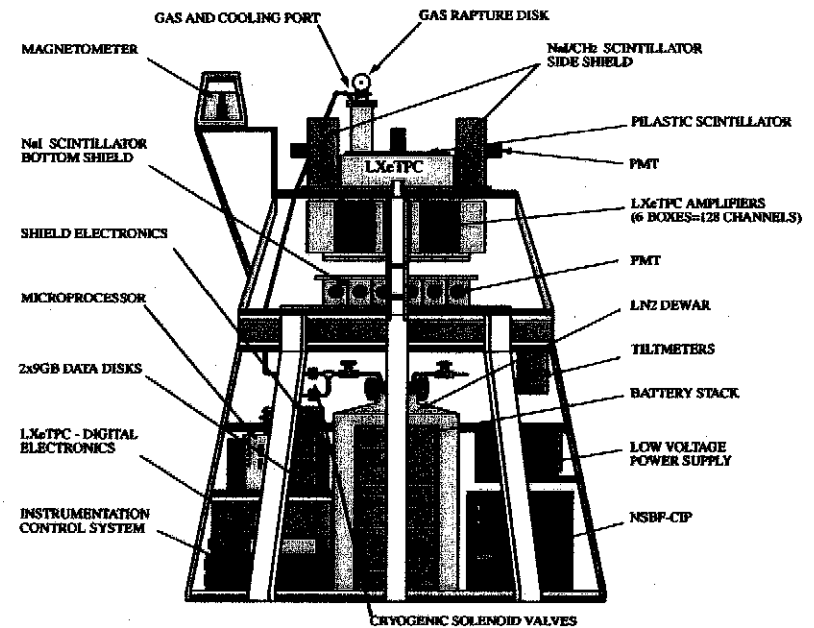
- Summer 1997: LXeGRIT first balloon flight and successful operation of a LXeTPC in space.
- Spring 1999: LXeGRIT stays afloat for 11 hrs. Instrument performs well despite the high data rate from low energy events.
- Fall 2000: LXeGRIT stays afloat for 27 hrs. TPC is operated without anticoincidence gamma or cosmic-ray shields, and with trigger optimized to MeV. Instrument performance is excellent. On going analysis of data from 27 hrs of observations (Crab, CygX-1, etc.) and from on ground calibration.



The LXeGRIT Gondola in Flight 2000 Configuration



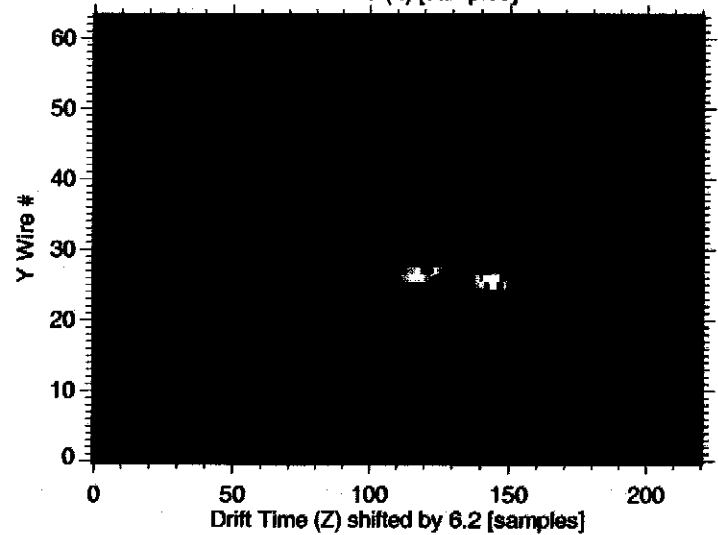
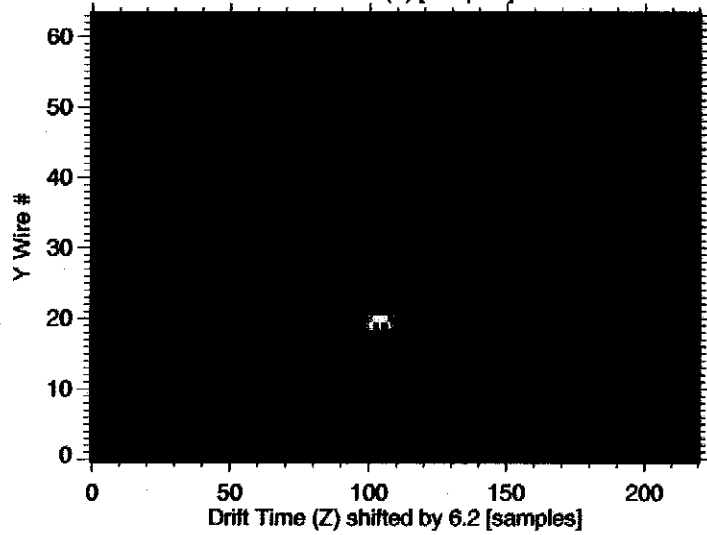
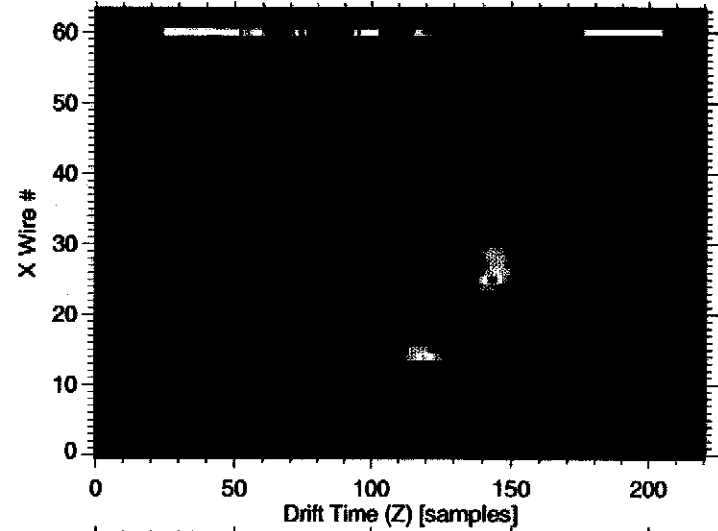
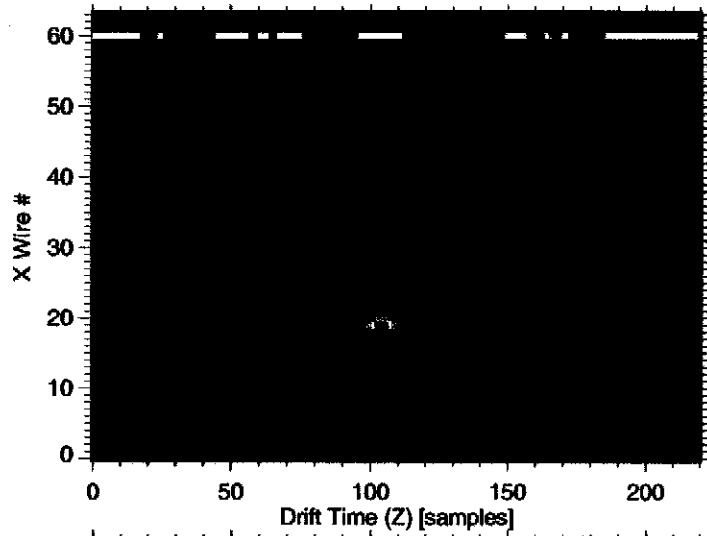
Detector	Liquid Xenon TPC
Active Volume	20 cm × 20 cm × 7 cm
Energy Range	0.1 – 10 MeV
Energy Resolution (FWHM)	$8.8\% \times (1 \text{ MeV}/E)^{1/2}$
Position Resolution (1σ)	1 mm (3 dimensions)
Angular Resolution (1σ)	3° at 1.8 MeV
Field of View (FWHM)	2 sr
Effective Area (Imaging)	20 cm² @ 1 MeV
Veto Shields	None
LN₂ Dewar	100 liter
Instrument Mass, Power	2000 lbs, 450 W
Telemetry, Onboard disks	2 × 500 kbps, 2 × 36 GB



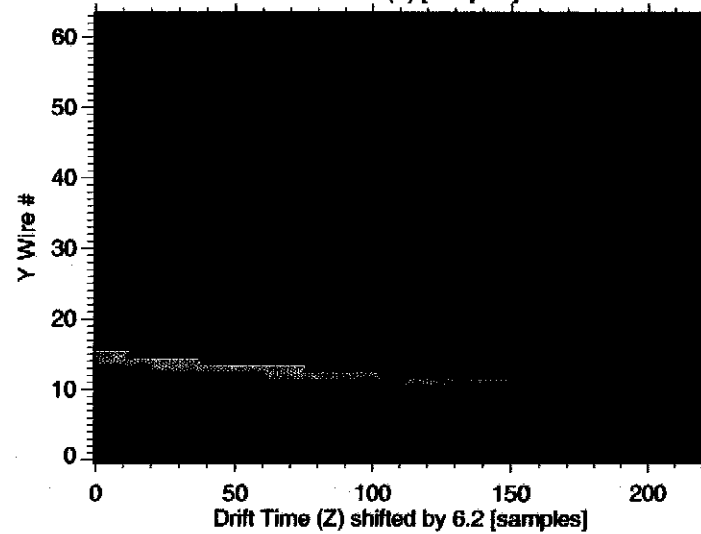
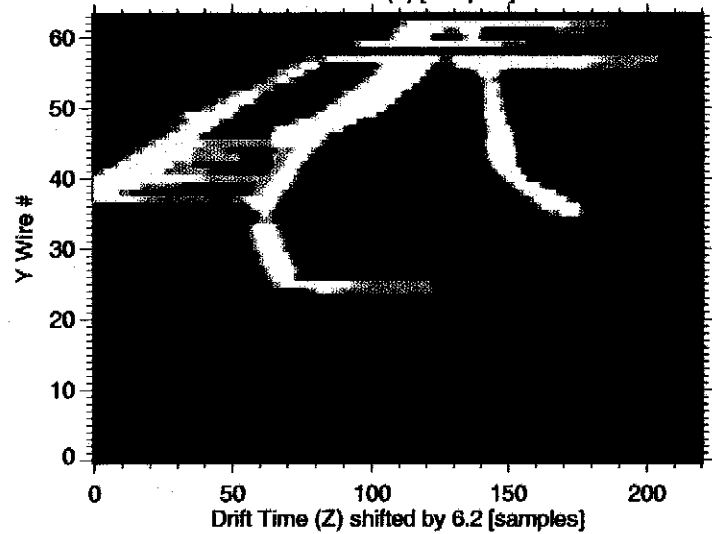
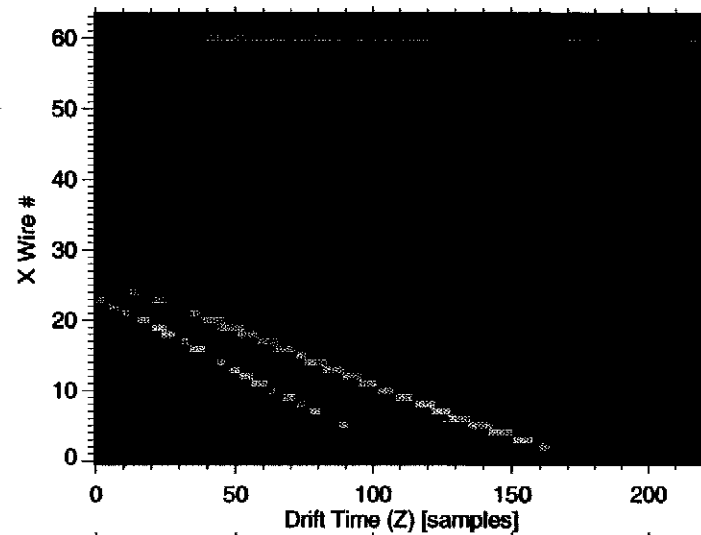
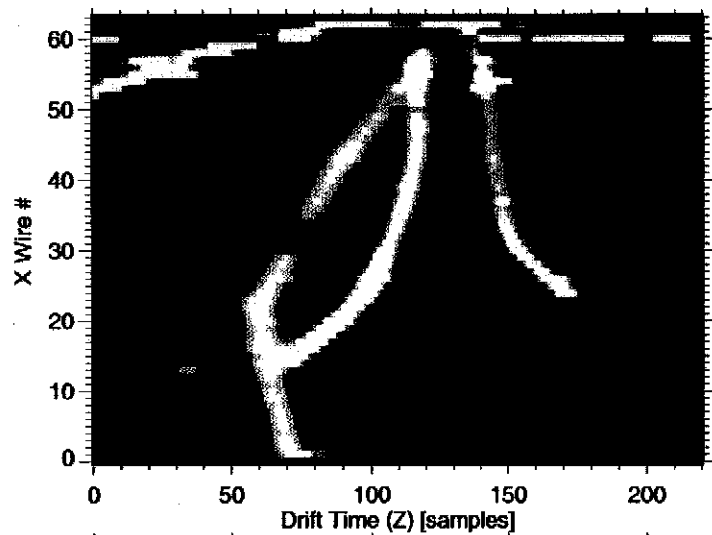
LXeGRIT in flight 1999 configuration

Event Imaging with LXeTPC:

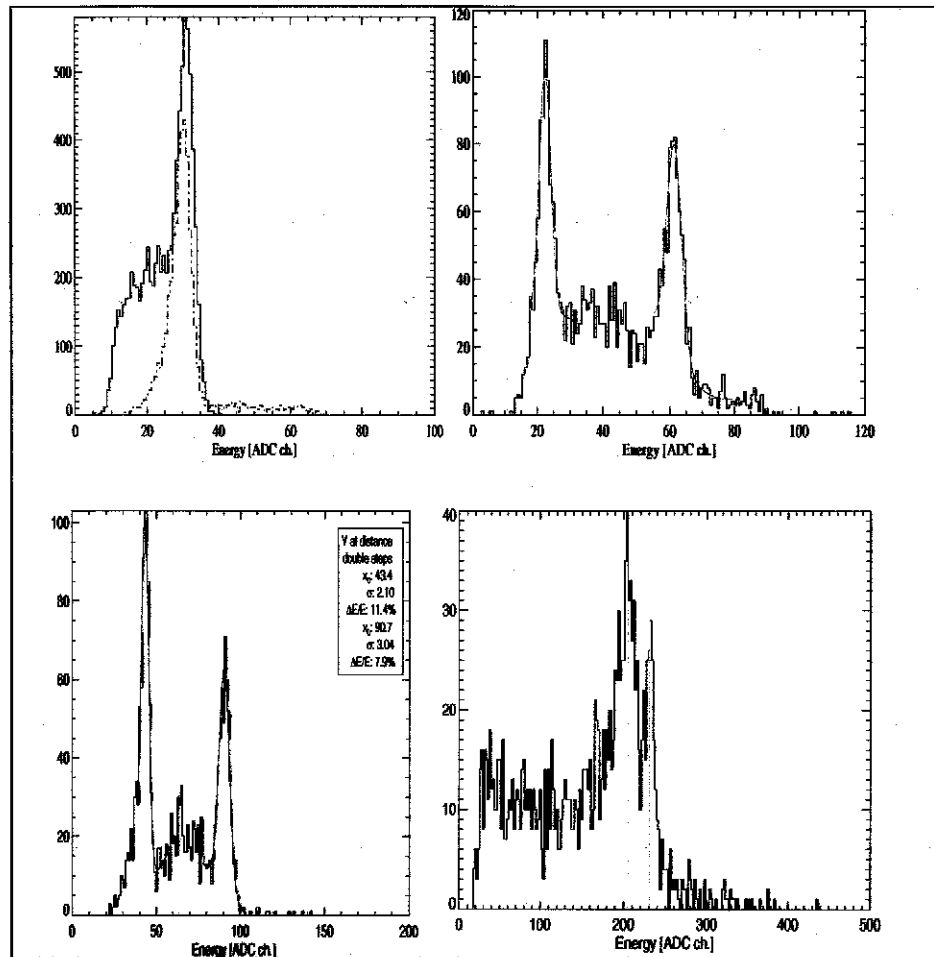
LXeGRIT 2000 – Flight Data – Gamma Rays



Event Imaging with LXeTPC: LXeGRIT 2000 – Flight Data – Charged Particles

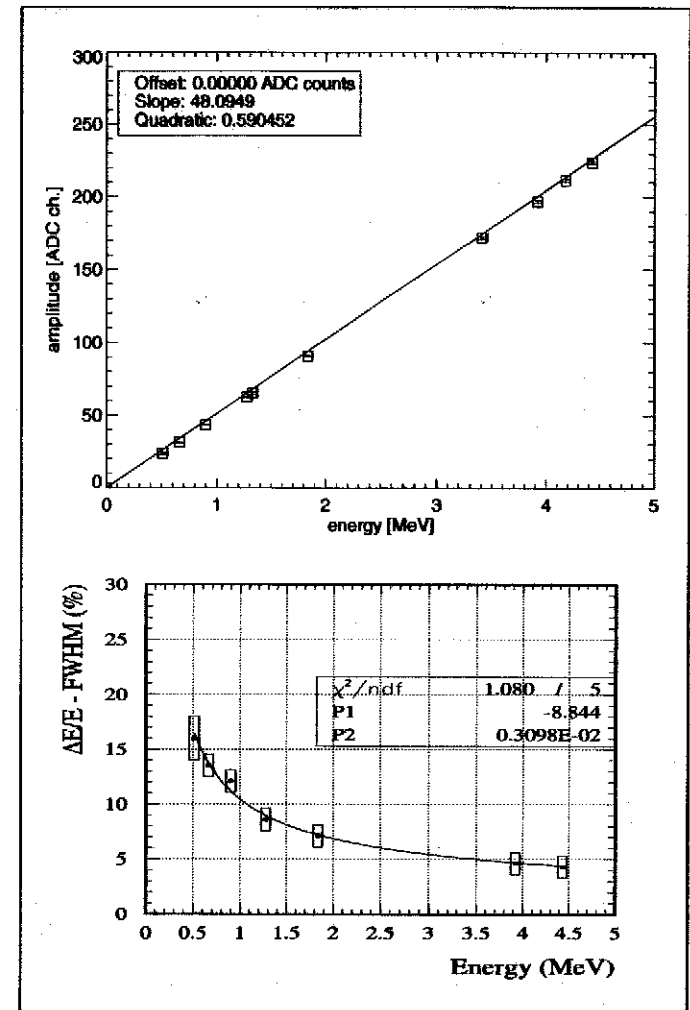


LXeGRIT Energy Calibration and Spectral Performance I



Energy Spectra – From top to bottom, clockwise:

^{137}Cs – 0.662 MeV: “1-step” (solid line) and “2-step” events (dashed red line), ^{22}Na – 0.511 and 1.275 MeV: “2-step” events, ^{88}Y – 0.898 and 1.836 MeV: “2-step” events, the source was placed about 2 m above the TPC, Am-Be: “2-step” events. The photopeak (4.43 MeV) and the single escape peak (3.92 MeV) are clearly identified.



From top to bottom:

Energy Calibration Curve:

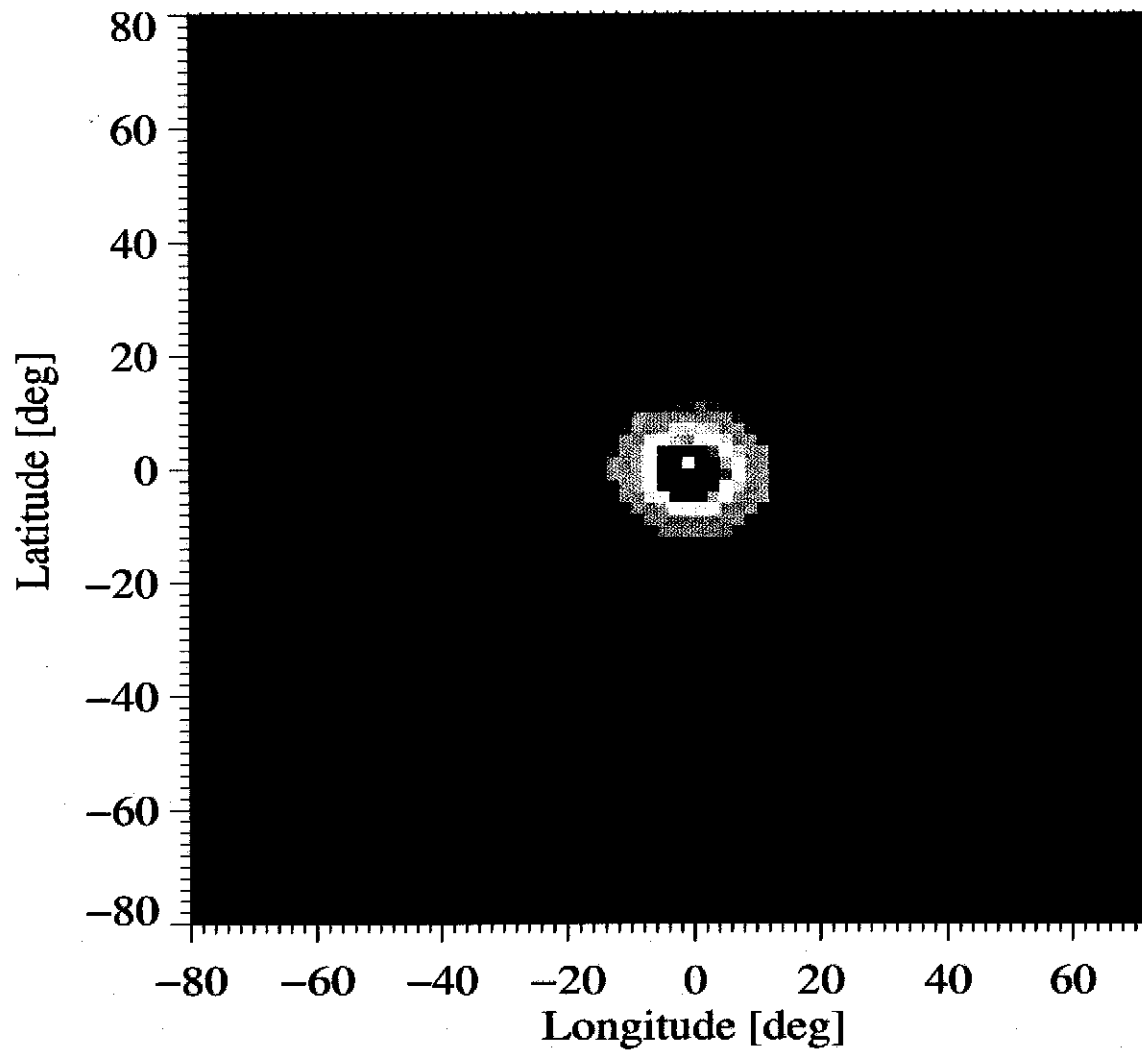
anode amplitude vs. energy

Energy Resolution vs. Energy:

$$\Delta E_{\text{LXe}}/E = 8.8\% \sqrt{1\text{MeV}/E}$$

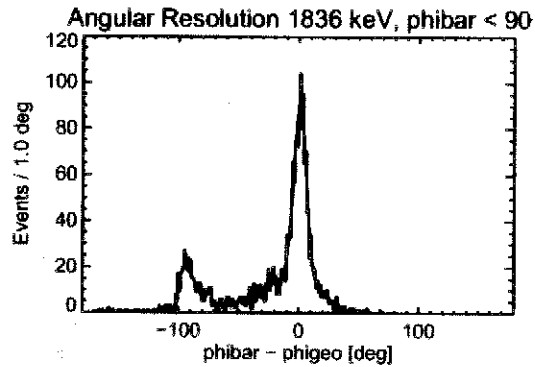
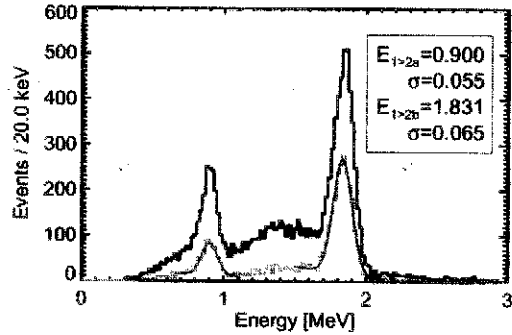
LXeGRIT Compton imaging performance

Reconstruction of the position of an ^{88}Y (1.8 MeV γ rays) source at distance using Compton events

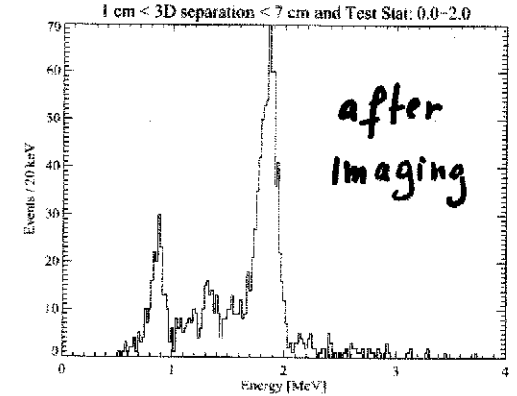
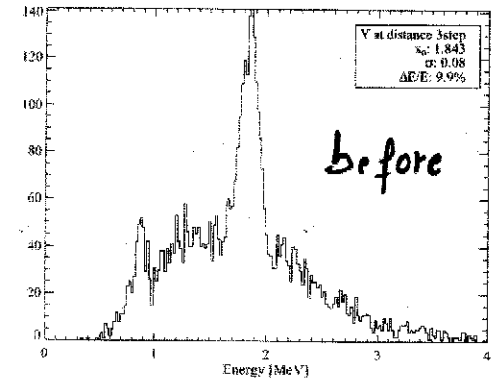
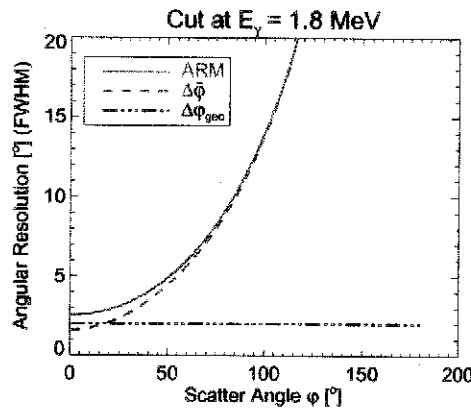


Imaging of an Y-88 Source on Oct. 3, 2000 with LXeGRIT on the Launchpad

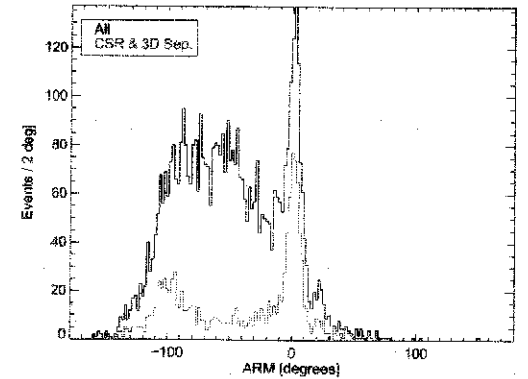
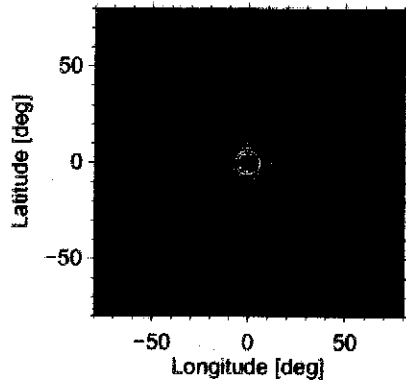
2-Step Events: Imaging by "larger step first".



3-Step Events:
Apply Compton kinematics for sequence reconstruction and background suppression.



ARM Image:



- LXeTPC with charge & light readout works as expected based on design parameters
- 3D event imaging and consequent background rejection demonstrated
- calibration and flight data analysis, together with MC simulations of instrument's response are providing the basis for the "next step"
- An optimized light readout and lower noise FE electronics currently being studied and designed - Will be implemented and tested in 2002 LXeGRIT balloon flight
- These upgrades will guide the implementation of the LXe technology for a next generation COMPTON telescope mission

New Scintillation Light Detection

Goal: Better light collection with reduced spread to achieve energy sensitivity on the trigger level

PMTs : Hamamatsu R6041 (Light in TPC, Gamma Rays)

R5900 (Light in Surrounding Volume, Background Shield)

- Very short design
- UV quartz window
- Bialkali photocathode
- Metal case for high pressure (> 3.5 atm)
- Tested at Liquid Xenon temperature (-100 C)
- Mounted within Liquid (no absorption in additional windows)

R5900

24 mm square window
10 stage multiplier

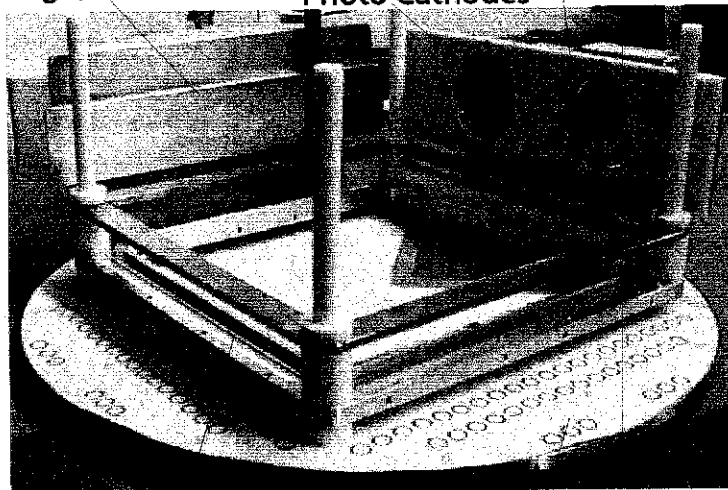
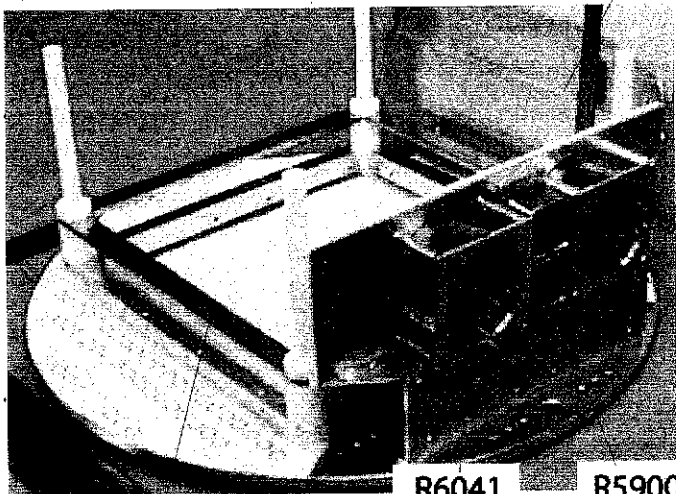
R6041

45 mm dia. photo cathode
12 stage multiplier

"Dummy Boxes"
(old design)

Teflon Relector

Photo Cathodes



R6041

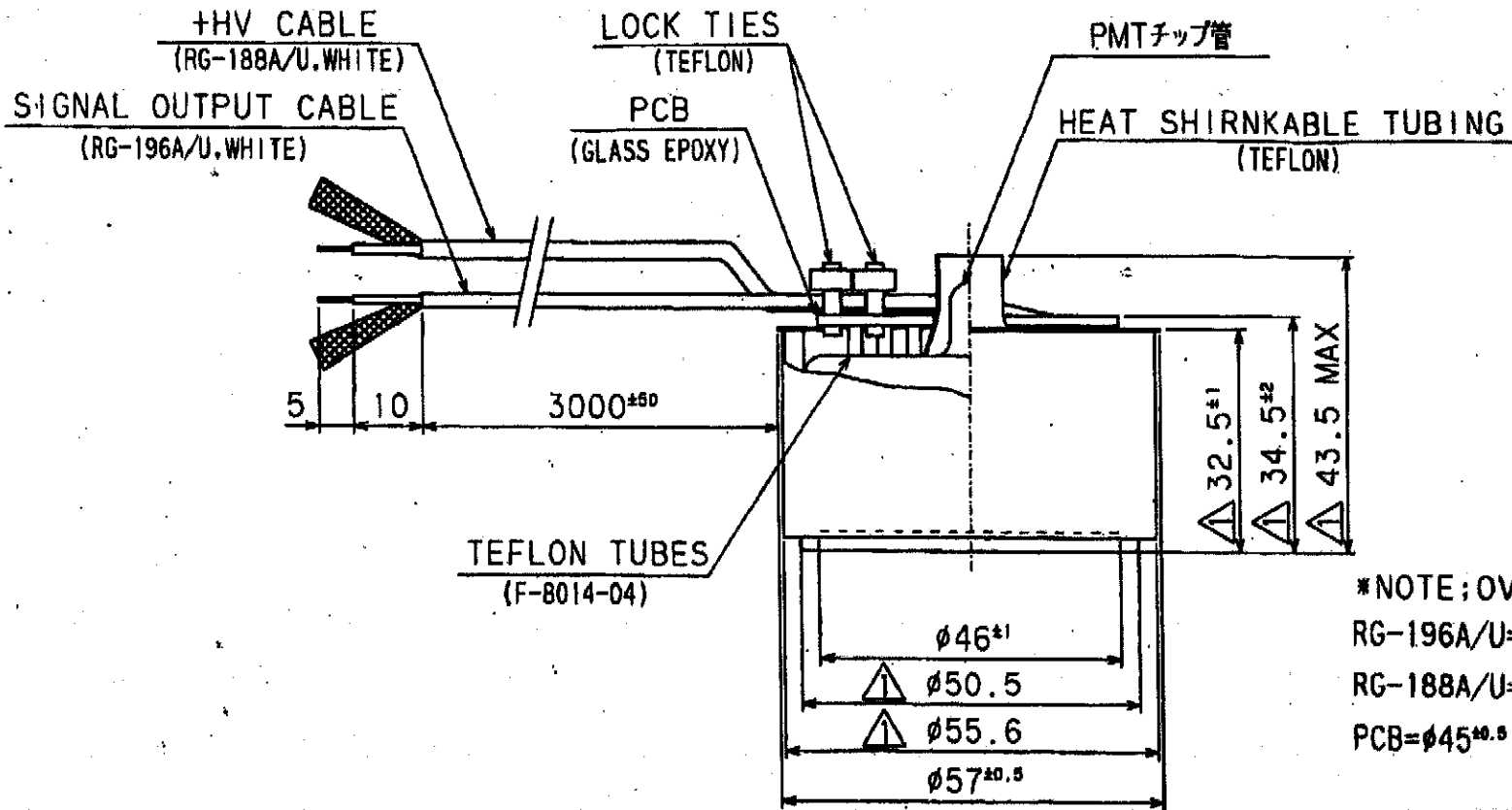
R5900

Anode and Wire Planes

Flange Mock-Up

Outline of TPC (Shaping Ring)

2000. 6. 2 10:00



*NOTE; OVERALL DIAMETER
 RG-196A/U=φ2.0(SIGNAL OUTPUT)
 RG-188A/U=φ2.6(+HV)
 PCB=φ45^{±0.5}

UNIT:mm

*REF TO DWG#5A-5843.

ITEM	NOTE	DATE	NAME	DIMENSIONAL OUTLINE	
				R6041Q ASSY (表面実装タイプ)	
△	PMTの改良による寸法変更	3 SEP'99		DRAWING NUMBER	5A-5843A
				DATE	3 SEP 1999
APPROVED BY: <i>[Signature]</i>			HAMAMATSU PHOTONICS K.K.		
CHECKED BY: <i>[Signature]</i>					
DRAWN BY: T. EMA	SCALE	1 / 1			

FROM

Prospects for a Next Generation Dark Matter Expt.

The LXeTPCs Array

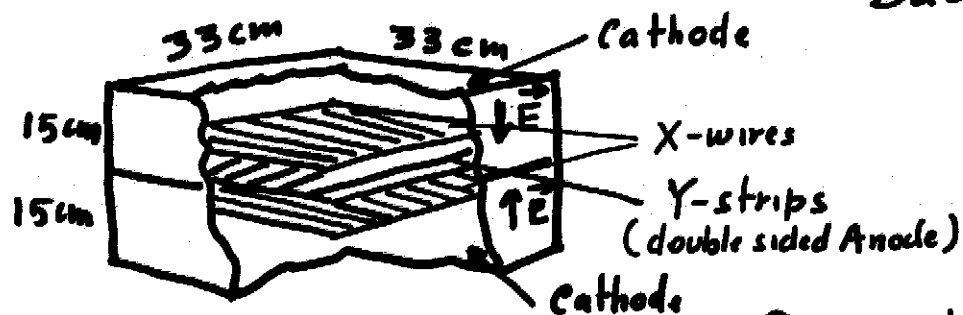
- Requirements:
- Sensitivity to $\leq 10^{-4}$ events / kg / day
 - Energy Threshold ≤ 10 keV
 - Background Rejection Efficiency $> 99\%$

- Implementation:
- Array of cryogenic LXeTPC modules with ionization + scintillation readout
 - internal + cosmogenic γ -induced & β -decay background identified & rejected via:

→ 3D event imaging

PSD of light signal

Active Shield of LXe scintillator



- unit module : 33 cm x 33 cm x 2 x 15 cm drift gaps
≈ 100 kg Active Xe target
+
~ 5 cm tick LXe active shield

R & D driven by DM application:

- low activity detector materials study
- high S/N for charge readout
 - optimize charge preamps AND/OR internal charge amplification with GEM
- high S/N for light readout
 - low activity version of Hamamatsu R6041 AND/OR CsI photocathodes AND/OR large area APDs
- optimize design with detailed MC studies

Columbia - led proposal to funding agency in preparation for submission this Fall -